"Mitomycin-Induced Pulmonary Veno-Occlusive Disease: Evidence From Human Disease and Animal Models."

Perros, Frédéric ; Günther, Sven ; Ranchoux, Benoit ; Godinas, Laurent ; Antigny, Fabrice ; Chaumais, Marie-Camille ; Dorfmüller, Peter ; Hautefort, Aurélie ; Raymond, Nicolas ; Savale, Laurent ; Jaïs, Xavier ; Girerd, Barbara ; Cottin, Vincent ; Sitbon, Olivier ; Simonneau, Gerald ; Humbert, Marc ; Montani, David

Abstract

BACKGROUND: Pulmonary veno-occlusive disease (PVOD) is an uncommon form of pulmonary hypertension characterized by the obstruction of small pulmonary veins and a dismal prognosis. PVOD may be sporadic or heritable because of biallelic mutations of the EIF2AK4 gene coding for GCN2. Isolated case reports suggest that chemotherapy may be a risk factor for PVOD. METHODS AND RESULTS: We reported on the clinical, functional, and hemodynamic characteristics and outcomes of 7 cases of PVOD induced by mitomycin-C (MMC) therapy from the French Pulmonary Hypertension Registry. All patients displayed squamous anal cancer and were treated with MMC alone or MMC plus 5-fluoruracil. The estimated annual incidence of PVOD in the French population that have anal cancer is 3.9 of 1000 patients, which is much higher than the incidence of PVOD in the general population (0.5/million per year). In rats, intraperitoneal administration of MMC induced PVOD, as demonstrated by pulmonary hypertension at right-h...

Document type : *Article de périodique (Journal article)*

Mitomycin-Induced Pulmonary Veno-Occlusive Disease
Evidence From Human Disease and Animal Models

Frédéric Perros, PhD; Sven Günther, MD; Benoit Ranchoux, PhD; Laurent Godinas, MD; Fabrice Antigny, PhD; Marie-Camille Chaumais, PharmD, PhD; Peter Dorfmüller, MD, PhD; Aurélie Hautefort, PhD; Nicolas Raymond, MSc; Laurent Savale, MD, PhD; Xavier Jaïs, MD; Barbara Girerd, PhD; Vincent Cottin, MD, PhD; Olivier Sitbon, MD, PhD; Gerald Simonneau, MD; Marc Humbert, MD, PhD; David Montani, MD, PhD

Background—Pulmonary veno-occlusive disease (PVOD) is an uncommon form of pulmonary hypertension characterized by the obstruction of small pulmonary veins and a dismal prognosis. PVOD may be sporadic or heritable because of biallelic mutations of the *EIF2AK4* gene coding for GCN2. Isolated case reports suggest that chemotherapy may be a risk factor for PVOD.

Methods and Results—We reported on the clinical, functional, and hemodynamic characteristics and outcomes of 7 cases of PVOD induced by mitomycin-C (MMC) therapy from the French Pulmonary Hypertension Registry. All patients displayed squamous anal cancer and were treated with MMC alone or MMC plus 5-fluoruracil. The estimated annual incidence of PVOD in the French population that have anal cancer is 3.9 of 1000 patients, which is much higher than the incidence of PVOD in the general population (0.5/million per year). In rats, intraperitoneal administration of MMC induced PVOD, as demonstrated by pulmonary hypertension at right-heart catheterization at days 21 to 35 and major remodeling of small pulmonary veins associated with foci of intense microvascular endothelial-cell proliferation of the capillary bed. In rats, MMC administration was associated with dose-dependent depletion of pulmonary GCN2 content and decreased smad1/5/8 signaling. Amifostine prevented the development of MMC-induced PVOD in rats.

Conclusions—MMC therapy is a potent inducer of PVOD in humans and rats. Amifostine prevents MMC-induced PVOD in rats and should be tested as a preventive therapy for MMC-induced PVOD in humans. MMC-induced PVOD in rats represents a unique model to test novel therapies in this devastating orphan disease. **(*Circulation*. 2015;132:834-847. DOI: 10.1161/CIRCULATIONAHA.115.014207.)**

Key Words: alkylating agents ■ antineoplastic agents ■ complications ■ drug-related side effects and adverse reactions ■ GCN2 ■ hypertension, pulmonary ■ pulmonary veno-occlusive disease

Pulmonary veno-occlusive disease (PVOD) is a rare and devastating cause of pulmonary hypertension (PH). PVOD is characterized by widespread fibrous intimal proliferation of septal veins and preseptal venules, and is frequently associated with pulmonary capillary dilatation and proliferation.[1] Although the pathology firmly confirms PVOD, a noninvasive diagnostic approach is usually favored in these fragile patients in whom a lung biopsy carries a high risk of life-threatening complications. Decreased diffusing capacity of the lung for carbon monoxide, severe hypoxemia, radiological abnormalities on high-resolution computed tomography (CT) scans of the chest, and the occurrence of pulmonary edema after starting pulmonary vasodilator therapy strongly argue for PVOD.[1,2] PVOD is a difficult form of PH to diagnose; it is frequently misclassified as idiopathic pulmonary arterial hypertension (PAH). Thus, the true incidence of PVOD is not known precisely, but is considered to represent 10% of cases of PAH

Clinical Perspective on p 847

Received October 2, 2014; accepted June 22, 2015.

From Univ. Paris–Sud, Faculté de Médecine, Kremlin-Bicêtre, France (F.P., S.G., B.R., L.G., F.A., P.D., A.H., N.R., L.S., X.J., B.G., O.S., G.S., M.H., D.M.); AP-HP, Centre de Référence de l'Hypertension Pulmonaire Sévère, Département Hospitalo-Universitaire (DHU) Thorax Innovation (TORINO), Service de Pneumologie, Hôpital de Bicêtre, Le Kremlin Bicêtre, France (F.P., S.G., B.R., L.G., F.A., A.H., L.S., X.J., B.G., O.S., G.S., M.H., D.M.); UMR_S 999, Univ. Paris–Sud, INSERM, Laboratoire d'Excellence (LabEx) en Recherche sur le Médicament et l'Innovation Thérapeutique (LERMIT), Centre Chirurgical Marie Lannelongue, Le Plessis Robinson, France (F.P., S.G., B.R., L.G., F.A., M-C.C., P.D., H.R., L.S., X.J., B.G., O.S., G.S., M.H., D.M.); Univ. Paris-Sud, Faculté de Médecine, Le Kremlin-Bicêtre, France (M-C.C.); Pulmonary Hypertension Research Group, Centre de Recherche de l'Institut Universitaire de Cardiologie et de Pneumologie de Québec, Université Laval, Canada (F.P.); Service de Pneumologie, CHU Mont-Godinne - Université Catholique de Louvain, Yvoir, Belgium (L.G.); AP-HP, Service de Pharmacie, Département Hospitalo-Universitaire (DHU) Thorax Innovation, Hôpital Antoine Béclère, Clamart, France (M-C.C.); Department of Pathology, Centre Chirurgical Marie Lannelongue, Le Plessis-Robinson, France (P.D.); and National Reference Centre for Rare Pulmonary Diseases, Department of Respiratory Medicine, Louis Pradel Hospital, Lyon, France (V.C.).

The online-only Data Supplement is available with this article at http://circ.ahajournals.org/lookup/suppl/doi:10.1161/CIRCULATIONAHA.115.014207/-/DC1.

Correspondence to David Montani, MD, PhD, AP-HP, Centre de Référence de l'Hypertension Pulmonaire Sévère, Service de Pneumologie et Réanimation Respiratoire, DHU Thorax Innovation, Hôpital de Bicêtre, 78, rue du Général Leclerc, 94270 Le Kremlin-Bicêtre, France. E-mail david.montani@bct.aphp.fr

that were initially considered as idiopathic or heritable, thus suggesting an incidence of <0.5/million per year.[2,3]

The pathophysiological mechanisms of PVOD remain poorly understood, in particular, because of the lack of animal models conducted on PVOD. PVOD may also be heritable and associated with biallelic mutations in the *Eukaryotic Translation Initiation Factor 2 Alpha Kinase 4 (EIF2AK4)* gene that codes for general control nonderepressible 2 protein (GCN2).[4] Isolated case reports suggest that chemotherapeutic agents may induce the development of PVOD.[5] However, PVOD is usually reported in patients receiving multiple regimens of chemotherapy, making it difficult to individualize drugs or pathophysiological mechanisms.

We have recently published systematic analysis and the experience of the French PH network, which suggests that alkylating agents may represent the predominant chemotherapeutic class of drugs associated with PVOD.[6] The French PH Network, which includes specialized pulmonary vascular centers, has now facilitated a study on the trends of PH and has developed a pharmacovigilance program at national level.[7–9] Since 2012, any cases of severe PVOD that have occurred in the setting of anal cancer and after therapy with mitomycin-C (MMC) have been identified in the French PH Registry and reported to the French pharmacovigilance agency. The present report summarizes the clinical characteristics and outcomes of 7 cases of MMC-associated PVOD identified in the French Registry. To confirm a causal link between MMC and human PVOD, we demonstrated that in rats, MMC induced specific remodeling of pulmonary venous and capillary compartments, representing a unique animal model of human PVOD. We have also demonstrated a preventive effect of amifostine, a cytoprotective agent, in animal models.[6]

Methods

Patients

We prospectively collected the clinical, functional, and hemodynamic characteristics and outcomes of PVOD associated with MMC therapy from the French PH Registry. The registry was established in accordance with the French bioethics laws (Commission Nationale de l'Informatique et des Libertés) and all patients gave their informed consent. Diagnosis of precapillary PH, defined as a mean pulmonary arterial pressure (mPAP) ≥25 mm Hg with a normal pulmonary capillary wedge pressure (PCWP) of ≤15 mm Hg, was confirmed in all patients by right heart catheterization. Right atrial pressure, mPAP, PCWP, and mixed venous oxygen saturation were recorded. Cardiac output (CO) was measured by using the standard thermodilution technique. Pulmonary vascular resistance was calculated as (mPAP–PCWP)/CO, expressed in Wood units. Acute vasodilator testing was performed during right heart catheterization by using inhaled nitric oxide, as previously described.[10] Routine evaluation at baseline included medical history, physical examination, echocardiography, high-resolution CT of the chest, ventilation/perfusion lung scan, abdominal ultrasound, autoimmunity screening, and human immunodeficiency virus (HIV) serology. Age at diagnosis, modified New York Heart Association functional class, and 6-minute walk distance were also recorded. All patients tested for *BMPR2* and *EIF2AK4* mutations received genetic counselling and signed written informed consent.

Number of cycles of MMC therapy, associated chemotherapeutic agents, delay between the last dose of MMC and diagnosis of PVOD, and outcomes were collected.

In Vivo Study Design

Rats were housed at the Faculty of Pharmacy of Châtenay-Malabry (ANIMEX platform, Châtenay Malabry, France). Experiments were conducted according to the European Union regulations (Directive 86/609 EEC) for animal experiments and complied with our institution's guidelines for animal care and handling. The animal facility is licensed by the French Ministry of Agriculture (agreement no. B92-019-01). This study was approved by the Committee on the Ethics of Animal Experiments CEEA26 CAP Sud. Animal experiments were supervised by Dr Frederic Perros (agreement delivered by the French Ministry of Agriculture for animal experiment no. A92–392). All efforts were made to minimize animal suffering.

Male and female Wistar rats (Janvier, 8 weeks old) were subjected to different protocols to evaluate sex differences, dose–response relationships, and the kinetics of PH development after MMC exposure.

Protocol 1: Sex-Specific Susceptibility

Male and female rats were randomly divided into saline (control, n=5) or MMC-exposed groups (Ametycin, Sanofi, 4 mg/kg IP, n=10). We performed hemodynamic measurements and assessed right ventricle hypertrophy, and tissues were collected at 24 days after the injection.

Protocol 2: Dose–Response Relationships

Females, which harbored a more severe response to MMC (than males), were used to study MMC-induced pulmonary vasculopathy induced by fractioned lower doses. Rats were randomly divided into saline (control, n=5) or MMC-exposed groups: ie, 2 and 3 $mg \cdot kg^{-1} \cdot wk^{-1}$ for 2 weeks (IP, n=10 for each dose). Rats were euthanized at 30 days after the first injection. Hemodynamic measurements were made, right ventricle hypertrophy was assessed, and tissue samples were collected.

Protocol 3: Kinetics of PH Development

Female rats were randomly divided into saline (control, n=5) or MMC-exposed groups (3 $mg \cdot kg^{-1} \cdot wk^{-1}$ for 2 weeks, IP, n=10). We evaluated the hemodynamics using echocardiography at baseline, and at 1, 2, 3, 4, and 5 weeks after the first MMC injection (n=5–10 rats for each time point).

Protocol 4: Prevention Study

Amifostine was given IP at 200 mg/kg 30 minutes before 3 $mg \cdot kg^{-1} \cdot wk^{-1}$ for2 weeks of MMC (n=15). This group was compared with the MMC-only exposed group (MMC, 3 $mg \cdot kg^{-1} \cdot wk^{-1}$ for 2 weeks, n=25). Survival was evaluated over 5 weeks. Survivors were euthanized at 5 weeks after the second MMC injection and assessed for hemodynamic, RV hypertrophy measurements, and tissue collection. For information about the choice of MMC doses used in this study, see the online-only Data Supplement.

Hemodynamic Measurements, Evaluation of Right Ventricle Hypertrophy, and Collection of Tissues

Rats were anesthetized with isoflurane (2 L/min O_2/3% isoflurane; Minerve, Esternay, France). Hemodynamic measurements were recorded with a PowerLab 4/35 data-acquisition system and analyzed with LabChart software (AD-Instruments, Oxford, UK).

In anesthetized rats, blood from the ventral-tail artery was taken for serum analyses before the hemodynamic measurements. A 3.5F umbilical-vessel catheter (Tyco, Plaisir, France) was introduced into the right external jugular vein. With the angle directed anteriorly, the catheter was inserted 2.5 cm proximally into the right atrium. The catheter was then rotated 90° anticlockwise and advanced 1 cm distally into the right ventricle (RV) and finally into in the pulmonary artery after an additional 1.5-cm advancement. Correct anatomic placement was confirmed by respective pressure contours. A T-type Ultra-Fast Thermocouple Probe (IT-23) was inserted into the left carotid artery to allow measurement of CO by the thermodilution technique, after the injection of cold saline into the pulmonary artery. Data mPAP in mm Hg, CO in mL/min, and total pulmonary resistances in Wood units were subject to statistical analyses.

Following exsanguination, the hilum of the left lung was ligated, and the right lung was distended by infusion of formalin via the trachea, and then embedded in paraffin. The noninflated left lung was snap-frozen in liquid nitrogen and used for protein quantification. The Fulton index for right ventricle hypertrophy, ie, the ratio of right

ventricular weight divided by left ventricular (LV) plus septal weight (RV/LV+S), was calculated.

Quantification of Pulmonary Microvessel Neomuscularization

Morphological assessment of pulmonary vascular remodeling is depicted in the online-only Data Supplement.

Hemodynamic Evaluation by Echocardiography

Rats were evaluated by transthoracic echocardiography (Vivid E9, GE Healthcare) by using a high-frequency transducer (12 S-D 4-12MHz, GE Healthcare). Evaluation was performed under general anesthesia and spontaneous breathing (isoflurane induction 4% at room air plus isoflurane maintenance 2% at room air). Pulmonary-artery acceleration time,[11] CO, and RV dilatation assessed by the ratio between the RV and LV and RV wall thickness were assessed according to guidelines from RV echocardiographic measurements.[12] All data were averaged during 5 cardiac cycles.

Histology and Special Stains

Hematoxylin-eosin, hematoxylin-eosin-safran, and orcein stains, and α-smooth muscle actin (clone 1A4, Sigma-Aldrich, Lyon, France) or proliferating cell-nuclear antigen (clone PC10, Dako, Les Ulis, France) immunohistochemical stains were applied to 5-µm-thick paraffin-embedded lung sections or 10-µm frozen sections by using a routine procedure.

Retrograde Microbead Injection From the LV

Following exsanguination, a catheter was introduced into the LV via the aorta and tied to the aorta. Then polystyrene microbeads (10 µm diameter; Polysciences, Warrington, PA), suspended in bovine serum albumin 20% (Sigma Aldrich, St-Louis, MO), was injected into the LV until the pulmonary veins became colored. The lungs were then inflated via the trachea with optimal cutting temperature compound diluted in phosphate-buffered saline, and then frozen in dry-ice–cold isopentane, as previously described.[13]

Proliferation Assay In Vivo

To examine cell proliferation in rats, we visualized the incorporation of exogenously supplied 5-ethynyl-2′-deoxyuridine (EdU) to identify cells that underwent DNA replication. EdU was injected intraperitoneally into the rats at 5 µg/g, at 72 hours before they were euthanized. EdU staining was performed by using a Click-iT EdU Alexa Fluor 488 Imaging Kit (Life Technologies, Saint Aubin, France) on frozen sections, according to the manufacturer's instructions. To characterize EdU-positive cells, we performed double immunostains with rabbit anti-CD34 (Ref ab81289, Abcam, Paris, France) and FITC-labeled anti-α-small muscle actin fluorescein isothiocyanate (clone 1A4, Sigma-Aldrich, Lyon, France) after EdU staining. Sections were viewed under a LSM 700 microscope (Carl Zeiss, Le Pecq, France) equipped with 405-, 488-, 555-, and 639-nm lasers (Carl Zeiss). Images were recorded and analyzed with ZEN software (Carl Zeiss).

Quantification of BMPRII and GCN2 Lung Expression by Western Blotting

Lung-tissue samples from rats and humans were prepared in lysis buffer containing 1% Igepal, 20 mmol/L Tris-HCl, 137 mmol/L NaCl, 10% glycerol, 2 mmol/L EDTA, 1 mmol/L Na_3VO_4, leupeptin 10 µg/µL, lepstatine 10 µg/µL, aprotinin 10 µg/µL, and a protease-inhibitor cocktail (aprotinin, leupeptin, and Pefabloc [Roche, Meylan, France]). Protein lysates (40 µg) were separated on sodium dodecyl sulfate polyacrylamide gel electrophoresis and transferred to a polyvinylidene fluoride membrane. After blocking, the membranes were incubated in Tris-buffered saline with Tween and 5% nonfat milk overnight at 4°C with the primary antibodies, BMPRII (Ref MA515827, 1/1000, Thermo Scientific), GCN2 (Ref 3302, 1/1000, Cell Signaling, Danvers, MA), and phospho-smad1/5/8 (Ref D5B10, 1/800, Cell Signaling), and the mouse monoclonal antibody against β-actin (Sigma), diluted to 1:2000. Blots were incubated with horseradish peroxidase–conjugated goat anti-mouse diluted to 1:10 000 (Cell Signaling) or with horseradish peroxidase–conjugated goat anti-rabbit diluted to 1:5000 (Cell Signaling), respectively. Antibodies were revealed by using enhanced chemiluminescence (Perkin Elmer). ImageJ software (http://rsb.info.nih.gov/ij/) was used to quantify the level of protein expression.

Construction of Network Pathways

We used Ingenuity Pathway Analysis (Qiagen, Redwood City, CA) as previously described.[14]

Statistical Analyses

Comparisons were made by using the Mann-Whitney (comparison between 2 groups) or Kruskal-Wallis (comparison between >2 groups) test, followed by the Dunn test. To compare the survival between the 2 groups, the log-rank test was used. P values of <0.05 were considered to be statistically significant.

Results

Description of MMC-Induced PVOD in the French PH Registry

We identified 7 cases of MMC-induced PVOD in the French PH Registry between June 2012 and December 2014. All patients presented with a diagnosis of squamous anal cancer; 2 of them were treated with MMC alone and 5 were treated with MMC plus 5-fluorouracil. A diagnosis of severe PVOD was definitively established in all patients based on clinical, functional, radiological, and hemodynamic characteristics (Table, Figure 1). All patients were tested for HIV infection, a common risk factor for PAH and anal cancer, and 1 test was positive (patient 2). No patient underwent a histological procedure because a lung biopsy was contraindicated in these fragile patients and lung transplantation was not proposed owing to the recent history of anal cancer.[1] The median age of patients was 53 years (range, 42–59) with a predominance of females (n=6). The delay between the end of chemotherapy with MMC and the diagnosis of PVOD was 4 months (range, 2–12 months). Patients received between 2 and 4 cycles of chemotherapy except for one who also received 8 cycles of 5-fluorouracil plus oxaliplatin (Table).

At diagnosis, patients with MMC-induced PVOD had severe clinical, functional, and hemodynamic symptoms. Patients were within New York Heart Association functional class III (n=4) or IV (n=3). Severe hypoxemia and a low diffusing capacity of the lung for carbon monoxide were observed in all patients (Table). Brain natriuretic peptide was increased at diagnosis in all patients (median, 951 ng/L; range, 452–1536 [normal value <100 ng/L]). Echocardiography suggested PH, impairment of RV function, and an absence of left heart dysfunction. Right-sided heart catheterization confirmed severe precapillary PH with a median mPAP of 41 mm Hg (range, 36–64 mm Hg), a decreased cardiac index of 2.1 $L \cdot min^{-1} \cdot m^{-2}$ (range, 1.6–4), and normal PCWP of <15 mm Hg in all patients. Median pulmonary vascular resistance was 11.2 Wood units (range, 5.5–13.6). High-resolution CT of the chest identified septal lines, centrilobular ground-glass opacities, and lymph enlargement in all patients (Figure 1). Pleural effusions were

Table. Characteristics of the 7 Patients With MMC-Induced PVOD Identified in the French PH Network

	Patient 1	Patient 2	Patient 3	Patient 4	Patient 5	Patient 6	Patient 7
Age at diagnosis, y	53	47	42	51	59	54	54
Sex, M/F	F	M	F	F	F	F	F
Delay between initiation of chemotherapy and PVOD, mo	5	6	4	2	4	4	12
Chemotherapy regimen	Mitomycin	Mitomycin 5-FU	Mitomycin 5-FU	Mitomycin	Mitomycin 5-FU	Mitomycin 5-FU	Mitomycin 5-FU Oxaliplatin
Number of cycles of mitomycin	3	2	2	4	4	2	11
NYHA functional class, I–IV	IV	III	III	IV	III	IV	III
6-MWD, m	Unable to perform	332	267	Unable to perform	240	Unable to perform	230
mPAP, mm Hg	41	36	39	64	46	37	43
PCWP, mm Hg	2	2	5	15	10	6	3
CI, $L \cdot min^{-1} \cdot m^{-2}$	2.1	1.6	2.8	3.5	4	1.9	2.1
PVR, WU	11.2	13.6	8.2	8.2	5.5	11.3	12.1
Svo_2, %	49	61	54	–	48	39.5	62
Pao_2, kPa (in room air)	6.1	7.7	NA	7.1	6.6	8.2 (5l/min O2)	7.1
DLCO, % theo	NP	21	30	36	51	NP	34
BNP, ng/L (<100 ng/L)	641	951	452	1536	1048	716	1279
Chest HRCT							
Septal lines	Yes	Yes	Yes	Yes	Yes	Yes	Yes
Ground-glass opacities	Yes	Yes	Yes	Yes	Yes	Yes	Yes
Lymph node enlargement	Yes	Yes	Yes	Yes	Yes	Yes	Yes
PAH therapy	ERA, PDE-5i	ERA, PDE-5i	ERA, PDE-5i	ERA	ERA, PDE-5i	ERA/ corticosteroids	Epoprostenol
Follow-up	Death from right heart failure	Death from severe pneumonia	Death from tumor progression and PH	Death from right heart failure	Alive after 3 mo	Alive after 3 wk	Alive after 12 mo
Mutations in *EIF2AK4* gene	No	–	No	–	–	No	No
Mutations in *BMPR2* gene	No		No			No	No

BMPR2 indicates bone morphogenetic protein receptor, type II; BNP, brain natriuretic peptide; CI, cardiac index; CO, cardiac output; DLCO, diffusing capacity of the lung for carbon monoxide; *EIF2AK4*, eukaryotic translation initiation factor 2 alpha kinase 4; ERA, endothelin receptor antagonists; 5-FU, 5-fluorouracil; HRCT, high-resolution computed tomography; NYHA, New York Heart Association; PCWP, pulmonary capillary-wedge pressure; PDE-5i phosphodiesterase type-5 inhibitors; PVOD, pulmonary veno-occlusive disease; RAP, right atrial pressure; 6-MWD, 6-minute walk distance; mPAP, mean pulmonary arterial pressure; PAH, pulmonary arterial hypertension; PVR, pulmonary vascular resistance; Svo_2, mixed oxygen saturation; and WU, Wood units.

present in 2 of the 7 patients, but no cardiac effusions were observed. Genetic screening for *EIF2AK4* and *BMPR2* mutations was performed in 4 patients, and identified no mutations. Because of the severely impaired hemodynamic parameters and the contraindication for lung transplantation, specific PAH therapies were introduced either as a monotherapy (n=2) or as a combination of endothelin-receptor antagonists and phosphodiesterase type-5 inhibitors (n=4) or prostacylins (n=1; Table). Diuretics were initiated in all patients.

A fatal course of the disease was observed in 4 of the 7 patients because of right heart failure (n=2), local tumor progression (n=1), and severe pneumonia (n=1).

Estimated Incidence of MMC-Induced PVOD in Patients With Anal Cancer in France

In cancer registries within France, the age-standardized incidence of squamous anal cancer is 0.2 to 0.7 per 100 000 cases per year in men, and 0.7 to 1.2 per 100 000 cases per year in women.[15] Thus, we estimated that a maximum of 600 new cases of anal cancer are diagnosed each year in France. In the French PH Network, we diagnosed 7 cases of MMC-induced PVOD in a 3-year period. The estimated incidence of PVOD in patients displaying anal cancer was 3.9 of 1000 patients per year and was higher than the incidence of PVOD in the general population, which is estimated at 0.5/million persons per year. The incidence of PVOD in the population that have anal cancer is, therefore, >5000 higher than in those with idiopathic PVOD. Indeed, not all patients that displayed anal cancer received MMC, which led to potential underestimation of the incidence of MMC-induced PVOD. Unfortunately, the exact number of patients treated with MMC in France was not available.

MMC-Induced PH in Rats With Pulmonary Vascular Lesions Resembling PVOD Lesions

When male and female rats were injected with a single dose of 4 mg/kg MMC, they developed PH. This was evident at 24 days later by a significant increase in mPAP, a decrease in CO, increased total pulmonary resistance, and compensatory

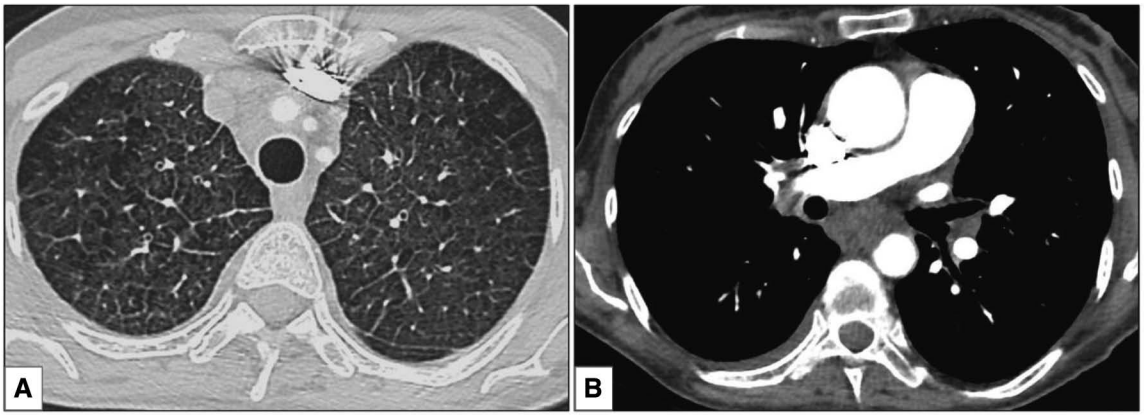

Figure 1. High-resolution CT of the chest in a patient displaying MMC-induced PVOD. **A**, Presence of septal lines and centrilobular ground-glass opacities. **B**, subcarinal lymphadenopathy. CT indicates computed tomography; MMC, mitomycin-C; and PVOD, pulmonary veno-occlusive disease.

RV hypertrophy, as quantified by the Fulton index (RV/(LV+S)) (Figure 2). Because of the small size of our experimental groups, we did not find a significant statistical difference between being male versus female using the log-rank test (data not shown). However, female rats seem to be more sensitive to the toxicity of MMC exposure because only a few (3/10) survived until the end point of the study (in comparison with 8/10 males surviving).

Specific lesions of human PVOD include septal-vein and preseptal-venule muscularization and fibrous occlusion; however, another important sign is focal capillary proliferation within the interstitium. In comparison with the controls (Figure 3A and 3B), we observed severe pulmonary vascular remodeling in rats with MMC-induced PH; this included (1) smooth muscle cell hypertrophy/hyperplasia in pulmonary arteries (Figure 3C), (2) neomuscularization of the small distal and normally not muscularized pulmonary vessels (Figure 3D), (3) vasculitis of the pulmonary arteries and veins (Figure 3E), (4) foci of pulmonary edema and capillaritis (Figure 3F and 3G), and (5) foci of alveolar wall thickening that resembled pulmonary capillary hemangiomatosis (Figure 3H).

Because female rats were more sensitive to MMC, we decided to treat females twice with lower doses (ie, 2 and 3 mg/kg) of MMC, at 1 week apart. Rats exposed twice to MMC were too fragile to undergo invasive hemodynamic measurements, so we evaluated the severity of PH by using the Fulton Index (Figure I in the online-only Data Supplement). At 30

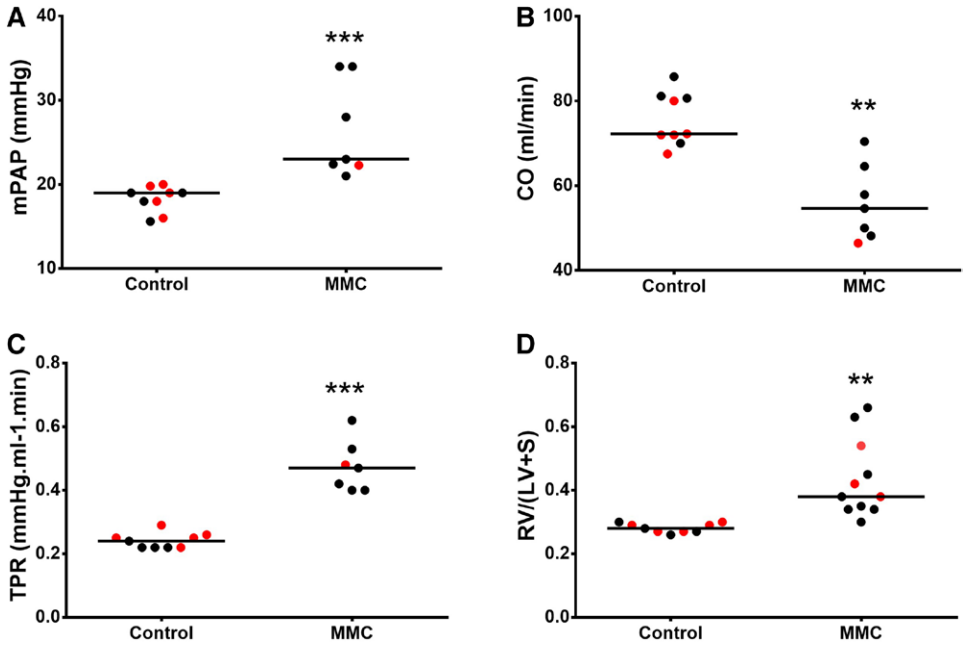

Figure 2. MMC induces PH in rat. **A**, Mean pulmonary arterial pressure (mPAP: in mm Hg) in control and MMC-exposed rats (MMC). **B**, Cardiac output (CO in mL/min). **C**, Total pulmonary vascular resistances (TRP: in mm Hg·mL^{-1}·min^{-1}). **D**, Right ventricular hypertrophy characterized by the Fulton Index (FI = right ventricle [RV]/left ventricle [LV] + septum [S] weight ratio). Black dots: males; red dots: females. Females were more sensitive to MMC than males: only 3 of 10 of females survived in comparison with 8 of 10 of males by day 24 after 4 mg/kg MMC. Because of the severe PH, we could only obtain hemodynamic data from 1 female. Dot plots with medians; ***P<0.001, ****P<0.0001. MMC indicates mitomycin-C; and PH, pulmonary hypertension.

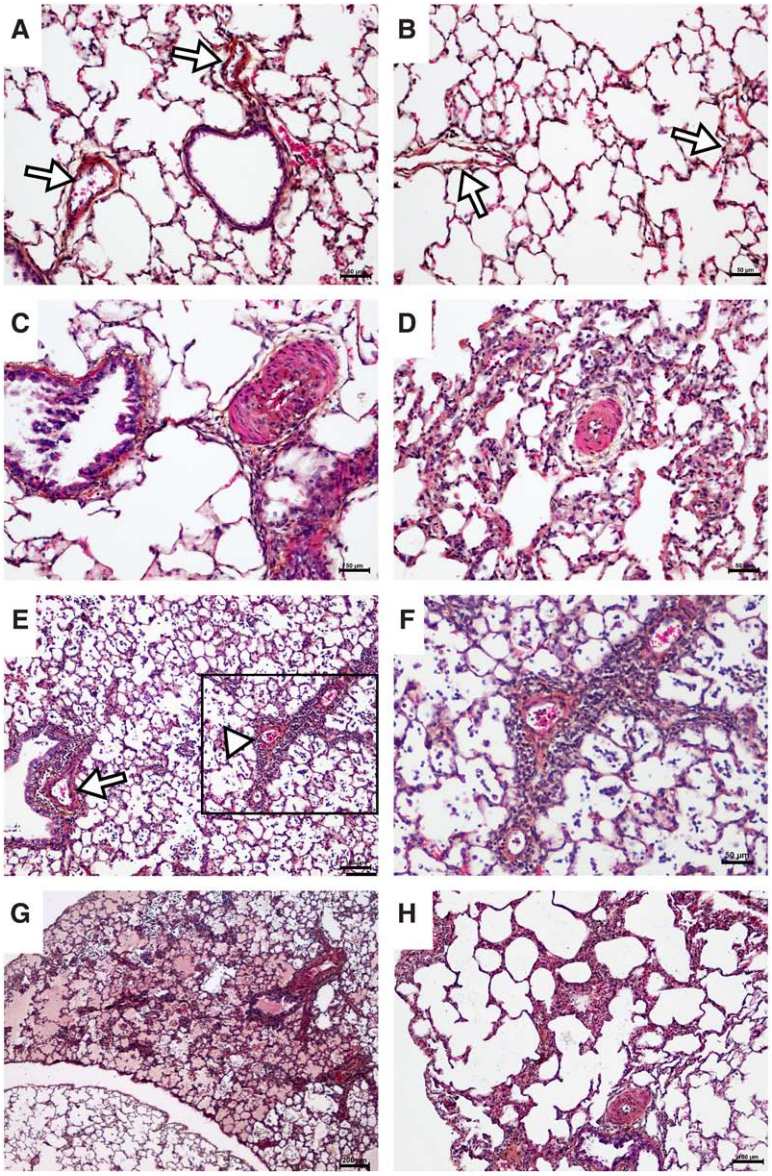

Figure 3. MMC induces pulmonary vascular remodeling in the rat, with significant pulmonary venous and capillary involvement that is highly suggestive of PVOD. **A** to **B**, Control lungs. **C** through **H**, MMC-exposed lungs. **A**, Control pulmonary arteries (arrows). **B**, Control distal microvessels (arrows, arterioles and venules are indistinguishable). **C**, Pulmonary artery with medial hypertrophy/hyperplasia. **D**, Neomuscularization of small distal, normally not muscularized, pulmonary microvessels. **E**, Vasculitis of pulmonary artery (arrow) and vein (arrowhead). **F** and **G**, Foci of pulmonary edema and capillaritis. **H**, Foci of alveolar wall thickening suggestive of pulmonary capillary hemangiomatosis. **A** through **H,** Hematoxylin-eosin-safran stained paraffin-embedded tissue sections. **A** through **D, G:** Scale bar, 50 μm. **E** and **H:** Scale bar, 100 μm. **F:** Scale bar, 200 μm. MMC indicates mitomycin-C; and PVOD, pulmonary veno-occlusive disease.

days after the first injection, female rats exposed to 3 mg/kg MMC had severe PH in comparison with controls and female rats given 2 mg/kg MMC. In animals that received 3 mg/kg MMC, we found severe obstructive lesions with pulmonary artery adventitial and intimal thickening, and medial hypertrophy/hyperplasia (Figure 4A through 4D). There was also intimal thickening and eosinophilic inflammation of pulmonary veins (Figure 4E through 4H). More distally, in the vessels accompanying the terminal bronchioles, we found medial hypertrophy of the small pulmonary arteries and severe intimal lesions of small pulmonary veins still associated with extensive adventitial accumulation of eosinophils (Figure 4M through 4P) in comparison with control vessels (Figure 5I through 5L). MMC-exposed arterioles (characterized by separated internal and external elastic lamina) and venules (characterized by a single external elastic lamina) arranged in the lung parenchyma harbored neomuscularization, neointimal thickening, and eosinophilic inflammation (Figure 4Q through 4S), as did the distal pulmonary arteries and veins. In contrast, microvessels (arterioles and venules) present in the control rats' parenchyma were indistinguishable (both were characterized by extremely thin walls; Figure 5T). The foci of pulmonary edema and capillaritis (Figure 4U and 4V) and the foci of alveolar wall thickening were suggestive of pulmonary capillary hemangiomatosis in the vicinity of the remodeled venule in MMC-exposed animals (Figure 4W and 4X): this strengthened the resemblance of this experimental model of PH to that of human PVOD.

To ascertain the postcapillary nature of the pulmonary microlesions found in MMC-exposed animals, we performed a retrograde injection of microbeads from the LV into the venous bed of the lungs. The 10-μm diameter of the beads did not allow them to cross the capillary bed. In control rats, bead-containing vessels displayed loose and slack walls and large lumens characteristic of veins and venules (Figure 5A through 5C). In MMC-exposed rats, the beads were plugged in severely remodeled microvessels, which we identified as postcapillary vessels (Figure 5D and 5F).

PVOD is characterized by numerous patchlike foci of capillary hemangiomatoses, which are produced by microvascular

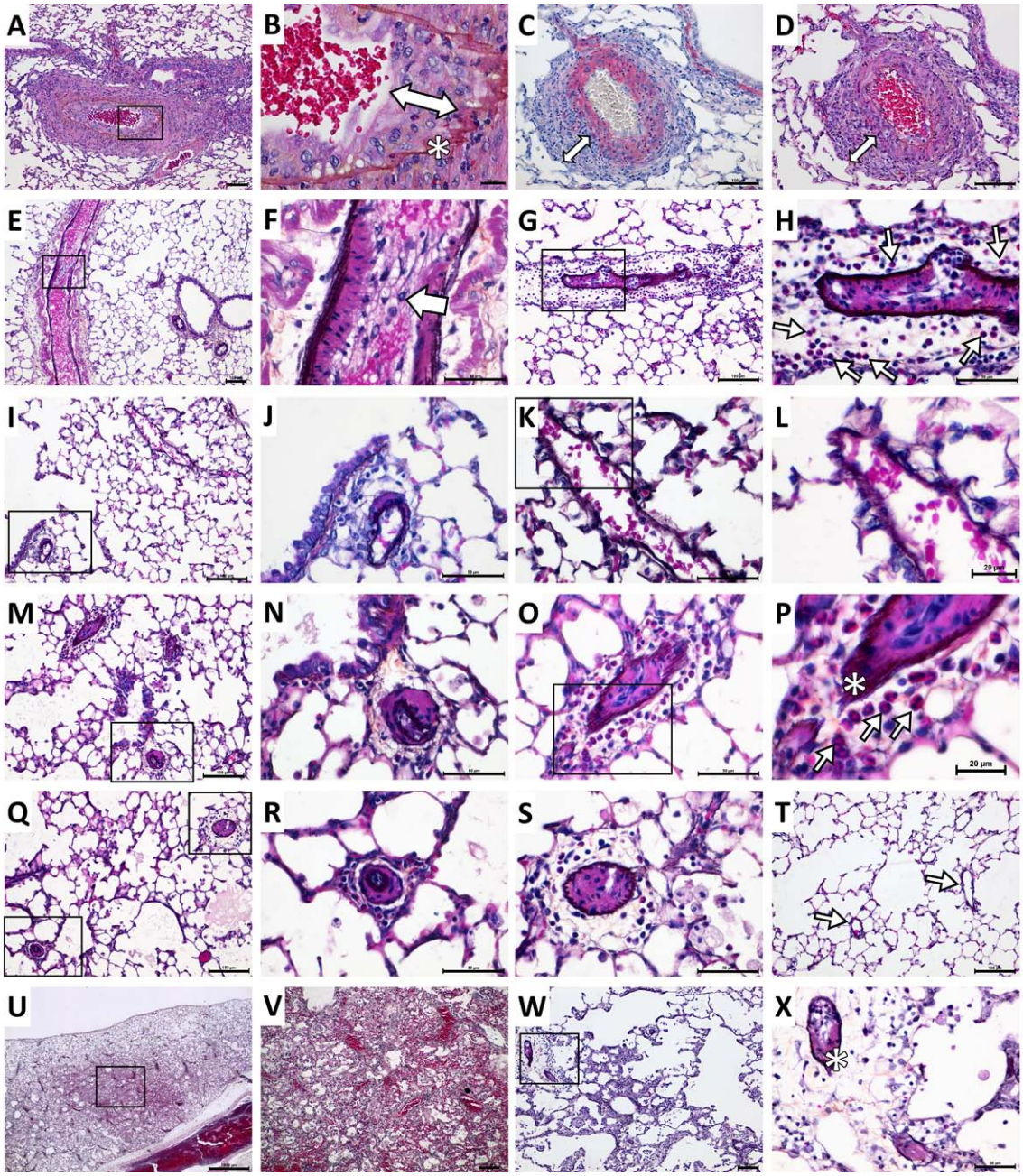

Figure 4. Rats exposed twice to 3 mg/kg MMC had severe pulmonary arterial, capillary, and venous remodeling; the histopathologic pattern of PVOD. **A** through **H**, **M** through **S**, and **U** through **X**, MMC-exposed lungs. **I** through **L** and **T**, Sex- and age-matched control lungs. **A** and **B**, Intimal remodeling (white double-headed arrow) of the muscular pulmonary artery accompanying the bronchus (external diameter >200 μm). Note the internal elastic (*). **C** and **D**, Adventitial remodeling (white double-headed arrow). Note the medial smooth muscle cells (α-smooth muscle actin, stained red; **C**) and fibrous remodeling of the adventitia (collagen in orange; **D**). **E** and **F**, Intimal thickening of pulmonary veins (external diameter >100 μm). **G** and **H**, Perivascular eosinophilic inflammation of the pulmonary vein (arrows). **I**, Control small pulmonary artery and vein (<100 μm). **J**, Control small pulmonary artery accompanying a terminal bronchiole with very thin muscular media. **K** and **L**, A small pulmonary vein with a typical thin loose, slack wall and a large lumen. **M**, A MMC-exposed small pulmonary artery accompanying a terminal bronchiole with hypertrophied muscular medium that is delimited by apparent internal and external elastica. **O** and **P**, A MMC-exposed small pulmonary vein, typically delimited by a single elastica, with severe lumen obstruction and extensive perivascular eosinophilic inflammation. **Q–S**, MMC-exposed arteriole (**R**) and venule (**S**) arranged in lung parenchyma and harboring neomuscularization, neointimal thickening, and eosinophilic inflammation, as were the distal pulmonary arteries and veins (**N**, **O**). **T**, Microvessels (arterioles and venules, *) present in the control parenchyma are indistinguishable. **U** and **V,** Foci of pulmonary edema and capillaritis. **W** and **X**, Foci of alveolar wall thickening suggestive of pulmonary capillary hemangiomatosis in the vicinity of the remodeled venule (*). **A**, **B**, **D** through **X**, Hematoxylin-eosin-safran + orcein staining, and **C,** α-smooth muscle actin immunostained paraffin-embedded tissue sections. **A**, **C**, **D**, **E**, **G**, **I**, **M**, **Q**, **T**, **U**, **W:** Scale bar, 100 μm. **F**, **H**, **J**, **K**, **N**, **O**, **R**, **S**, **X:** Scale bar, 50 μm. **B**, **L**, **P:** Scale bar=20 μm. **U:** Scale bar, 1000 μm. MMC indicates mitomycin-C; and PVOD, pulmonary veno-occlusive disease.

endothelial-cell proliferation (Figure 6B), and was almost undetectable in the control rats' lung parenchyma (Figure 6A). To examine cell proliferation in rats, we visualized the incorporation of exogenously supplied EdU to identify cells undergoing DNA replication. In control lung parenchyma, we observed very few EdU-positive cells (Figure 6C), whereas

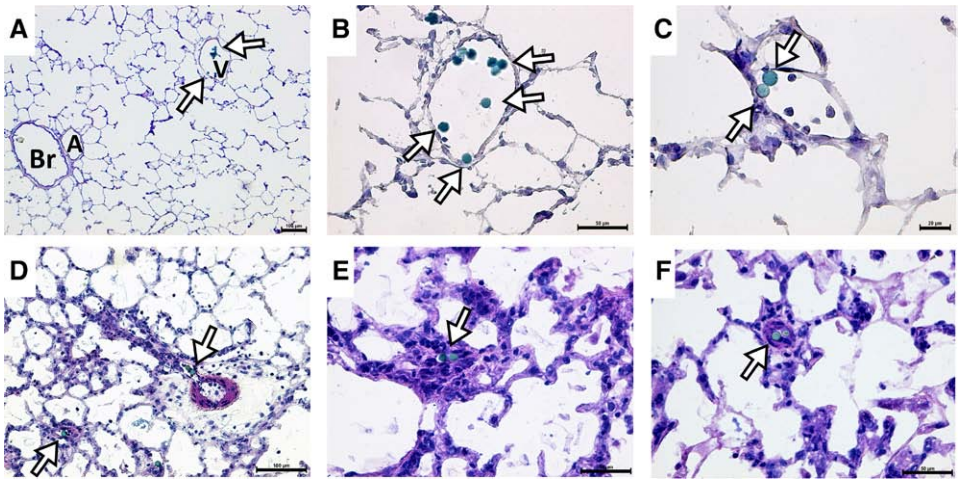

Figure 5. Identification of veins and venules by retrograde injection of microbeads from the left ventricle. **A** through **C**, Control lungs. **D** through **F**, MMC-exposed lungs. **A**, Large field of a control lung. Br indicates bronchus; A, artery; and V, vein. Only the vein contains green beads. **B** and **C**, Control venules with green beads. Control venules display a loose and slack wall and a large lumen. **D**, **E**, and **F**, Vein and venules of MMC-exposed lungs. Beads allow identification of severely remodeled vessels as postcapillary vessels. **A** through **F**, Hematoxylin-eosin–stained frozen sections. **A** and **D:** Scale bar, 100 μm. **B**, **E**, and **F:** Scale bar, 50 μm. **C:** Scale bar, 20 μm. MMC indicates mitomycin-C.

there was a focus of intense microvascular endothelial-cell proliferation (parenchymal CD34+EdU+ cells) in MMC-exposed rats (Figure 6C through 6G). We also saw endothelial (luminal CD34+EdU+ cells) proliferation in pulmonary venules, which was identified by the presence of microbeads (retrograde injection) in the lumen (Figure 6E). We also observed adventitial-cell proliferation in the remodeled pulmonary microvessels of these animals (Figure 6D and 6F).

Kinetics of MMC-Induced PH in Rats

To assess the time course of PH development in MMC-exposed rats, we performed echocardiographic analyses at the time of MMC injection and then weekly for the 5 weeks. Pulmonary artery acceleration time was significantly reduced from the fourth week onward in comparison with the controls (medians, 25 versus 39 ms, P=0.0007) and baseline values (medians, 25 versus 30 ms, P=0.0035). CO was significantly

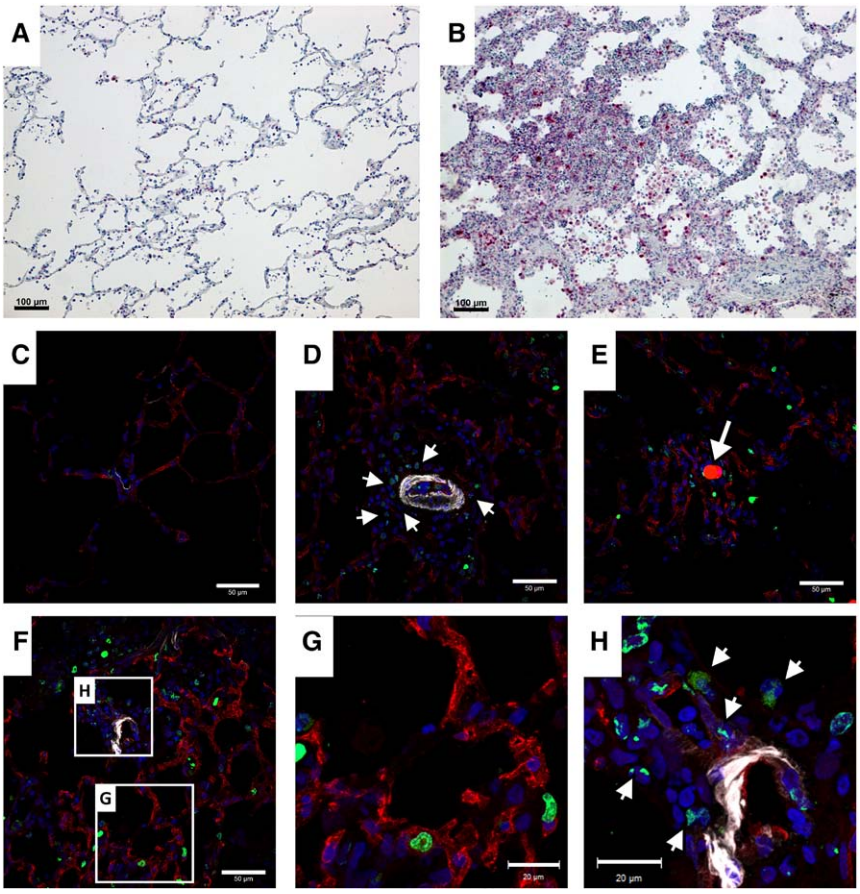

Figure 6. Microvascular endothelial cell (MEV) proliferation in human PVOD and MMC-induced PVOD-like PH in rats. **A** and **B**, Human lungs, PCNA IHC stains (red stain=proliferating cells; blue counterstain, hematoxylin) on paraffin-embedded tissue sections. **C** through **G**, Rat lungs, click-iT EdU stain (green nuclei=proliferating cells) with CD34 (endothelial cells, in red) and α-smooth muscle actin (smooth muscle cells/α-SMA, in white) immunofluorescent staining of frozen sections and confocal imaging. Counterstain=4′,6-diamidino-2-phenylindole (DAPI). **A**, Control human lung parenchyma displays very little cellular proliferation. **B**, Pulmonary capillary hemangiomatosis (PCH) from explanted PVOD lung is characterized by intense MEV proliferation. **C**, Control rat-lung parenchyma displays very little MEV proliferation. **D** through **G**, PCH-like foci from MMC-exposed rats display intense MEV proliferation (red cells with green nucleus). Note the microvessels coated with α-SMA (neomuscularization) displaying adventitial-cell proliferation (arrows); the venule is identified by the red autofluorescent microbead (*, retrograde injection), and displays important endothelial-cell proliferation. **A** and **B:** Scale bar, 100 μm. **C** through **F:** Scale bar, 50 μm. **G:** Scale bar, 20 μm. EdU indicates 5-ethynyl-2′-deoxyuridine; IHC, immunohistochemistry; MMC, mitomycin-C; PCNA, proliferating cell-nuclear antigen; and PVOD, pulmonary veno-occlusive disease.

reduced from the fourth week in comparison with the controls (medians, 73 versus 110 mL/min, P=0.0008) and baseline values (medians, 73 versus 91 mL/min, P=0.0056). The RV wall thickness was significantly increased in comparison with control (medians, 0.08 versus 0.06 cm, P=0.0187) and baseline values (medians, 0.08 cm versus 0.06 cm, P=0.0047). The ratio of RV to LV increased from the fifth week in comparison with baseline values (medians, 0.58 versus 0.52, P=0.0326). For some animals, we managed to have both echo readings and direct hemodynamic measurement by catheterization: both gave comparable results (Figure II in the online-only Data Supplement).

MMC-Induced PVOD in Rats With Reduced GCN2 Expression and Disruption of smad1/5/8 Signaling

On the one hand, our group demonstrated that *EIF2AK4* (coding GCN2) is the major gene linked to PVOD[4]; on the other hand, *BMPR2* mutations are strongly related to PAH susceptibility/development.[16] We measured the protein expression of these 2 genes in MMC-exposed rats. We found that the pulmonary protein level of BMPRII was unaffected in these animals, whereas protein levels of GCN2 were decreased (Figure 7A). Moreover, we found that GCN2 pulmonary protein levels were inversely related to the dose of MMC exposure: a high dose of MMC was related to higher PH and lower GCN2 levels (Figure 7B). Accordingly, explanted lungs from heritable PVOD showed null expression of GCN2, whereas BMPRII levels remained not statistically different from the control lungs (Figure 7C).

Although the pulmonary protein level of BMPRII was unaffected in MMC-exposed rats and in human PVOD, both conditions were characterized by an almost total disruption of smad1/5/8 signaling (Figure 7D and 7E). Because the dysfunction of GCN2 signaling is crucial to the development of PVOD, we wondered if this pathway could modulate the smad cascade in the absence of BMPRII alteration, and thus explain, at least in part, our results. We used Ingenuity Pathway Analysis software, a Web-based mammalian biology knowledgebase and analysis tool used for genomic data analysis, to decipher the connections between both signals. We found a complex and unrevealed interplay between both signals (Figure III in the online-only Data Supplement).

Amifostine Prevented PVOD Development When Used in Combination With MMC

Amifostine ameliorated MMC-induced PVOD with notable improvement in survival (Figure 8A), RV hypertrophy (Figure 8B), and pulmonary hemodynamics (increase in CO with a decrease in total peripheral vascular resistance) in MMC + amifostine-treated rats (Figure 8C through 8E). The decrease of total pulmonary resistance in MMC + amifostine–treated rats was linked to a decrease in resistive fully muscularized distal microvessels, and an increase in low-resistance nonmuscularized distal microvessels (Figure 8F through 8H). The percentage of occluded distal microvessels was significantly lowered in the amifostine group (Figure 8I).

Discussion

Since 2012, the French PH Network has identified 7 cases of PVOD in patients treated with MMC for squamous anal cancer, which is the major indication for MMC in France. These PVOD patients typically present with precapillary PH, radiological abnormalities seen on high-resolution CTs of the chest, a low diffusing capacity of the lung for carbon monoxide, and severe hypoxemia. These patients had severe symptoms and marked hemodynamic symptoms at diagnosis. According to previous reports, the prognosis of these PVOD patients appeared very poor, and 4 of 7 seven patients died shortly after diagnosis of acute right heart failure or tumor progression.[17–19] Indeed, 2 of the 7 patients received only MMC, which strongly reinforced the hypothesis of a direct link between MMC and PVOD. Nevertheless, these findings should not obscure the possibility that several other drugs may also have had similar effects as MMC. A recently published analysis of the association between chemotherapeutic agents and PVOD suggests that alkylating agents may represent a drug class at risk for PVOD.[6]

In France, treatment with MMC is nearly exclusively used in the setting of anal cancer. Therefore, we used the number of patients treated in France for this indication and extrapolated these results to obtain an incidence rate for PVOD after exposure to MMC. The lower estimated incidence of PVOD in patients displaying anal cancer is excessively high (3.9/1000 per year) in comparison with the incidence of PVOD in the general population (<1/million per year). However, MMC-induced PVOD has also been reported in the setting of non–small-cell lung cancer,[18] gastric adenocarcinoma,[20] and cervical carcinoma.[5] MMC lung toxicity is mainly caused by acute or chronic interstitial lung diseases, with an estimated incidence of 1.8%.[21]

In this study, we have confirmed the role of MMC in the development of pulmonary vascular lesions in animal models. In rats, MMC exposure induced pulmonary hypertension with pulmonary vascular lesions that resembled PVOD lesions: ie, (1) foci of alveolar wall thickening suggestive of pulmonary capillary hemangiomatosis, (2) foci of pulmonary edema and capillaritis, (3) vasculitis of pulmonary veins and arteries, (4) intimal and adventitial remodeling of pulmonary arteries and veins (especially after 2 exposures to MMC), (4) neomuscularization of small distal pulmonary microvessels, (5) venule obstruction, and (6) medial hypertrophy/hyperplasia of pulmonary arteries. The postcapillary nature of the pulmonary microlesions found in MMC-exposed animals was ascertained through retrograde injection of microbeads from the LV into the venous bed of the lungs. Subsequently, the beads became plugged into severely remodeled microvessels of treated rats, and were identified as postcapillary vessels. MMC-exposed lungs also displayed foci of intense microvascular endothelial-cell proliferation, mimicking the patchlike foci of capillary hemangiomatosis found in PVOD. We also observed endothelial and adventitial cell proliferation in the remodeled pulmonary microvessels of these animals.

We assessed the time course of PH development in MMC-exposed rats through echocardiographic analyses at the time of MMC injection, and then every week for 4 weeks. Echocardiographic abnormalities appeared from the fourth

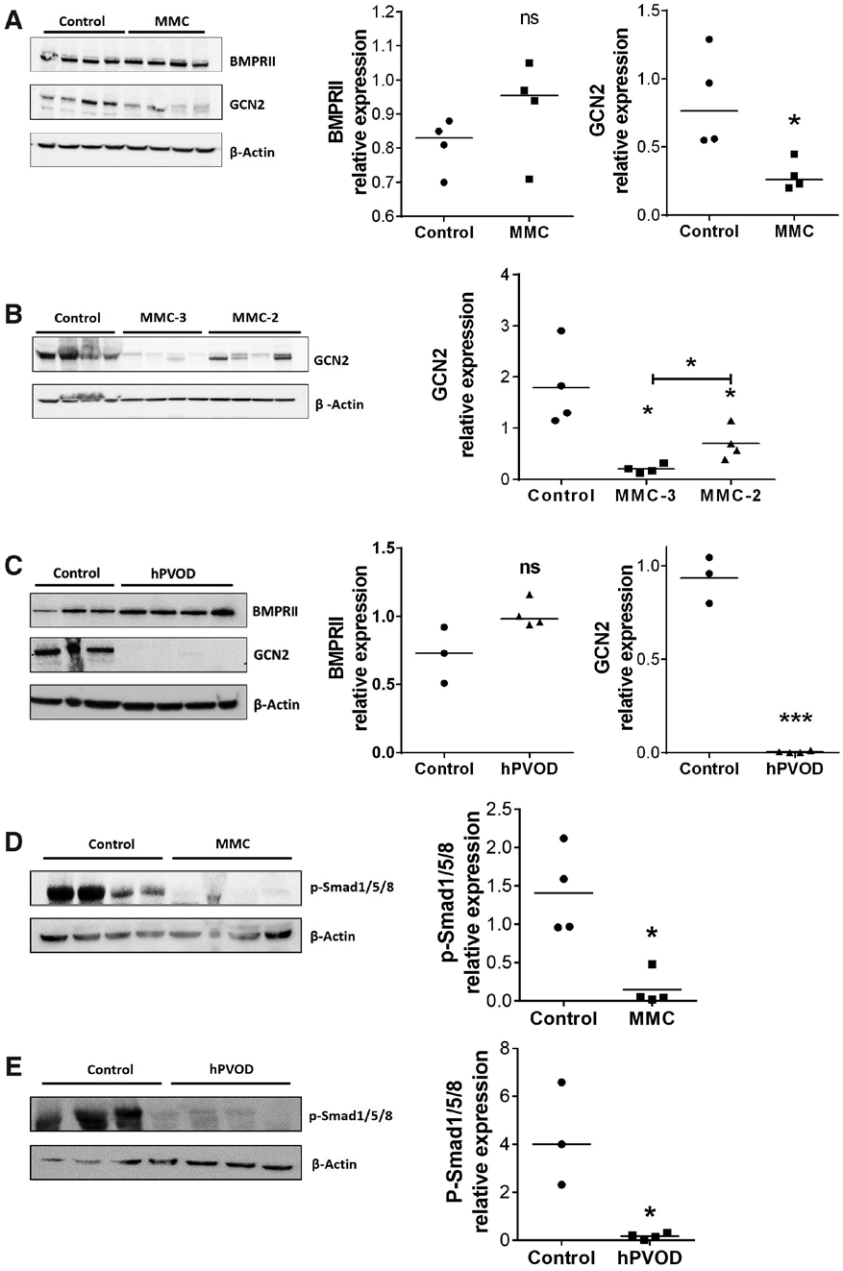

Figure 7. Pulmonary levels of BMPRII GCN2 and p-smad1/5/8 in human PVOD and MMC-induced PVOD-like PH in rats as measured by Western blot analysis (WB). β-Actin was used as loading control. Right panels: quantification of the WBs. **A**, BMPRII and GCN2 protein expression in lungs from controls or rats exposed to a single dose of MMC (4 mg/kg). **B**, GCN2 protein expression in lungs from controls or rats exposed to 2 low (2 mg/kg) or high (3 mg/kg) doses of MMC. **C**, BMPRII and GCN2 protein expression in lungs from controls or human heritable PVOD (hPVOD) explanted lungs. **D**, p-smad1/5/8 phosphoprotein expression in lungs from controls or rats exposed to a single dose of MMC (4 mg/kg). **E**, p-smad1/5/8 phosphoprotein expression in lungs from controls or hPVOD explanted lungs. Box Plot (Min to Max); **P*<0.05, *****P*<0.0001, n=3–4/group. MMC indicates mitomycin-C; PH, pulmonary hypertension; and PVOD, pulmonary veno-occlusive disease.

week of follow-up. Females were more susceptible to MMC toxicity. Interestingly, although the female/male (F/M) ratio for anal cancer is 2:1 in the general population in France,[15,22] the sex disequilibrium for MMC-induced PVOD was much stronger (F/M ratio: 6:1). Of note, the only man affected in our series was also HIV infected, a risk factor for both PAH and anal cancer, whereas all 6 women were HIV negative. Even if there is no pathophysiological explanation to date, experimental and human data suggest an increased susceptibility of females to MMC-induced PVOD. The reasons for the association between female sex and MMC toxicity are poorly understood.

Only a small proportion of patients who received MMC (alone or in combination with other chemotherapeutic agents) will develop PVOD, although all the rats developed pulmonary venous remodeling in this study. This observation is in accordance with the low proportion of patients who develop PAH in other forms of drug-induced PAH (appetite suppressants, <1/10 000[23]; dasatinib, <1/100[24]), suggesting an individual susceptibility to pulmonary vascular drugs. In our series, 5 patients received MMC with 5-fluorouracil and 1 patient had a comorbid HIV infection, a well-known cause of PAH. We cannot exclude that multiple hits may explain the development of PVOD in these patients. Nevertheless, the occurrence of PVOD in 2 patients receiving only MMC (without any other known PAH risk factors) and the data obtained in animal models, suggest a direct role of MMC in pulmonary venular lesions. The multiple hits hypothesis has also been proposed in other pulmonary vascular diseases such as drug-induced PAH or heritable PAH. This susceptibility is not explained by mutations in *EIF2AK4* gene[4] in our patients. These results do not exclude the involvement of other genetic characteristics

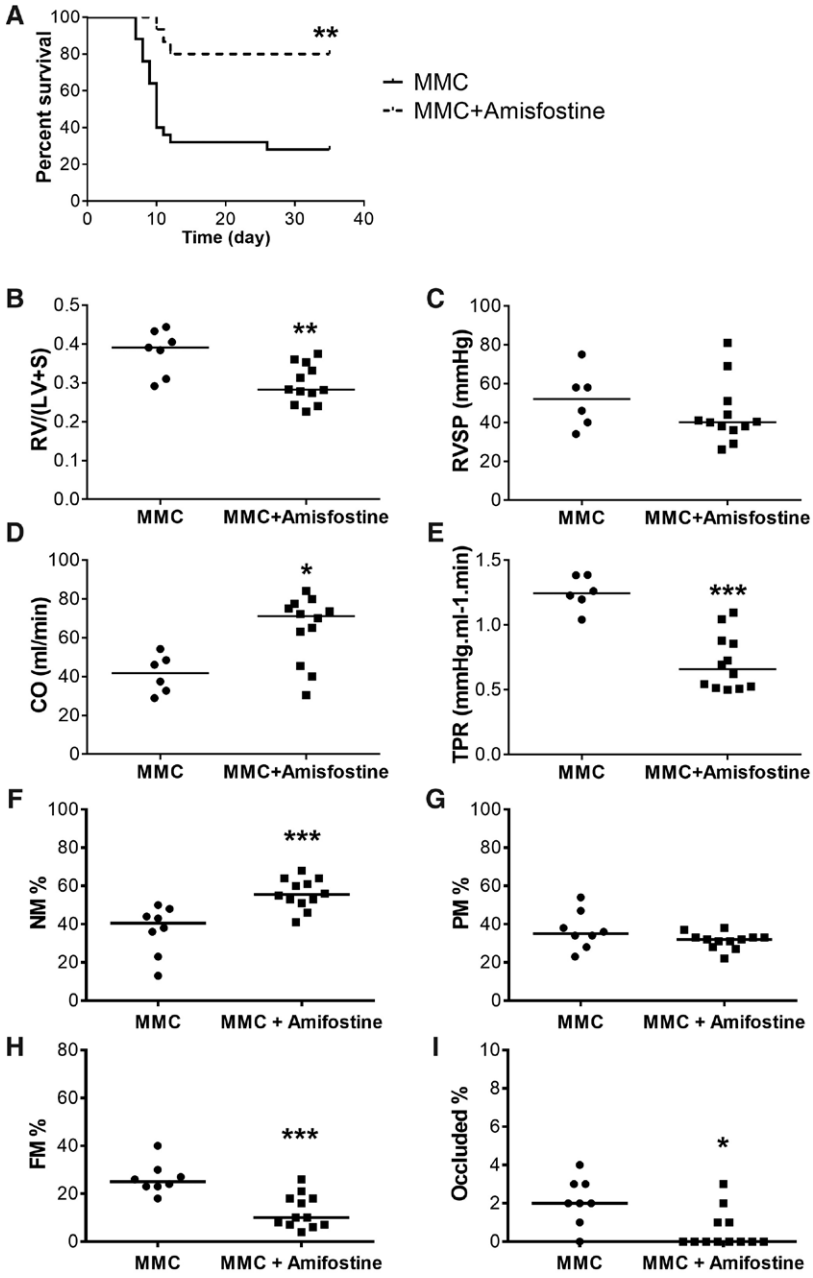

Figure 8. MMC-induced PVOD is partially prevented by amifostine pretreatment. Amifostine was given IP at 200 mg/kg for 30 minutes before 3 $mg \cdot kg^{-1} \cdot wk^{-1}$ for 2 weeks of MMC. Animals were euthanized at 4 weeks after the second MMC injection. Survival, right heart hypertrophy and hemodynamic parameters were evaluated. **A**, Survival curves for MMC, and MMC + amifostine groups. **B**, Fulton Index (FI = right ventricle [RV]/ left ventricle [LV] + septum [S] weight ratio). **C**, Right ventricular systolic pressure (RVSP) in mm Hg. **D**, Cardiac output (CO) in mL/min. **E**, total pulmonary resistances (TPR) in $mm\,Hg \cdot mL^{-1} \cdot min^{-1}$. MMC-induced pulmonary vascular remodeling is alleviated by amifostine pretreatment. Muscularization of distal vessels (DV; <50 μm) was evaluated. **F**, % of nonmuscularized (NM) DV. **G**, % of partially muscularized (PM) DV. **H**, % of fully muscularized (FM) DV. **I**, % of occluded DV. Dot plots with medians; **P*<0.05, ***P*<0.01, *****P*<0.0001. MMC indicates mitomycin-C; and PVOD, pulmonary veno-occlusive disease.

and particular susceptibility polymorphisms in other genes. It is well accepted that several risk factors, such as gene mutations, autoimmunity, drugs, and infection, may induce PAH. Similarly, we hypothesize that PVOD could result from different triggers, including chemotherapeutic agents, connective tissue disease (such as systemic sclerosis), or genetic susceptibility (biallelic *EIF2AK4* mutations).

We cannot exclude that an associated treatment, such as chemoprotectant (amifostine) or corticosteroids, may also modulate pulmonary vascular injury and reduce the side effects of MMC toxicity in patients. None of our patients received amifostine. To investigate preventive strategies, we evaluated the impact of amifostine in MMC-induced PVOD in rats. In this animal model, amifostine markedly improved survival and significantly decreased pulmonary distal vascular remodeling, total pulmonary resistance, RV hypertrophy, and RV function. These experimental data suggest that cytoprotective agents may have an ability to prevent PVOD in patients treated with MMC.

Interestingly, we demonstrated in animal models that MMC induced a PVOD-like disease and depletion of pulmonary GCN2 content in a dose-dependent manner. Although the pulmonary protein level of BMPRII was unaffected in MMC-exposed rats and in human PVOD, both conditions were characterized by almost total disruption of smad1/5/8 signaling. Using Ingenuity Pathway Analysis, we found a complex and unrevealed interplay between both signals, which improves our understanding of PH/PVOD pathobiology and justifies further investigations.

PVOD patients have a poor outcome, with a worse prognosis than PAH patients. To date, there is no cure for this devastating disease, and the use of specific PAH therapies

(prostacyclin, endothelin-receptor antagonists, or phosphodiesterase type 5 inhibitors) may induce life-threatening pulmonary edema.[1,2,25,26] Thus, the benefits of these treatments have not been demonstrated in PVOD; the only recommended treatment is lung transplantation for eligible PVOD patients.[1,2,27] MMC-induced PVOD in rats represents a specific model for pulmonary venous involvement associated with reduced GCN2 expression; this suggests that it could represent a general model for idiopathic, heritable, or drug-induced PVOD. Indeed, this model constituted a unique opportunity to learn more about the pathophysiology of PVOD and to test an innovative therapy.

MMC is an alkylating agent with antibiotic and antitumor characteristics. It has been previously used to treat pancreatic, stomach, and breast cancers; however, anal cancer remains the main indication for this drug therapy.[28] Complications from this treatment are bone marrow toxicity, renal damage, and interstitial lung diseases, caused by extensive tissue damage. Pulmonary vascular injuries, including alterations to endothelial cells, have also been reported.[29] MMC-related lung toxicity is a dose-dependent side effect.[30] It was thought that MMC could have selective toxicity on cancer cells through specific tumor expression of MMC-activating enzymes, such as NAD(P)H:quinone oxidoreductase (NQO1). NQO1 is a flavoenzyme that catalyzes the 2-electron reduction of quinones and related compounds, such as MMC. NQO1 has been shown to be overexpressed in many types of cancer. However, Siegel et al[31] also demonstrated a high level of NQO1 protein expression in normal lung respiratory epithelium and pulmonary vascular endothelium. Hence, vascular cells in normal lungs contain marked NQO1 protein expression and may be damaged by MMC therapy, leading to specific pulmonary vascular toxicity.[31]

The development of lung damage induced by MMC begins with irregular thickening of the endothelial cells of the capillaries and progresses to the release of a surfactant and to the activation of alveolar macrophages.[32] In a woman treated with MMC plus 5-fluorouracil, who developed progressive and fatal PH, scanning electron microscopy of the cast blood vessels showed distortion and destruction of alveolar capillaries that prohibited the passage of erythrocytes. Extensive capillary damage and venous occlusion were observed, resulting in excessive new capillary formation, sometimes in angiomatoid configurations, and hypertrophy of pulmonary veins and arteries.[33] At the molecular level, it has been suggested that MMC-induced pulmonary vascular dysfunction may be related to its bifunctional alkylating property. Cultured pulmonary-artery endothelial cells exposed to MMC showed similar growth arrest and morphological alterations to monocrotaline pyrrole, another bifunctional alkylating substance known to be a potent trigger for experimental PH in rats.[29,34] Both alkylating agents may compromise the capacity for replicative repair of endothelial cells, accounting for the delayed vascular injury induced by these molecules. Moreover, it has been shown that MMC results in a marked decrease in the biosynthesis of prostacyclin in cultured human umbilical cord vein endothelial cells.[35] Last, MMC has the characteristics expected of a bioreductive alkylating agent: activation of alkylating species occurs more readily under hypoxic conditions, and the drug is selectively cytotoxic to hypoxic cells.[36] The underlying hypoxic condition may thus increase the pulmonary vascular side effects of MMC.

Biallelic mutations of the *EIF2AK4* gene (coding GCN2) have been identified as the predisposing gene related to heritable PVOD.[4] According to our results, we can hypothesize that MMC depletes GCN2 in the lungs and mimics PVOD induced by *EIF2AK4* mutations. Interestingly, Wilson et al[37] have demonstrated that the loss of GCN2 promotes oxidative stress and inflammatory-mediated DNA damage during asparaginase therapy; this suggests that patients with reduced GCN2 may be at risk of developing hepatic complications during asparaginase treatment. Our results may suggest that MMC-induced GCN2 depletion could favor similar oxidative and inflammatory pulmonary injuries.

Recently, Lathen et al[38] demonstrated that the ERG–APLNR axis may play a role in the control of pulmonary-venule endothelial proliferation. These authors demonstrated that *Erg* binds to and serves as a transcriptional activator of the G-protein–coupled receptor gene, *Aplnr*, and that the knockout of either *Erg* or *Aplnr* results in pulmonary venous–specific endothelial proliferation in vitro.[38] Indeed, mice with a homozygous deletion of *Erg* or *Aplnr* develop remodeled postcapillary pulmonary venules. Interestingly, in human PVOD lung tissues, levels of ERG protein, APLNR-mRNA, and protein were significantly decreased in comparison with control lungs.[38] Unlike our animal model of MMC-induced PVOD, which was characterized by a dose-dependent depletion in pulmonary GCN2 content, the authors did not find any difference in the expression of GCN2 in lung tissues from animals with homozygous or heterozygous deletion of *Erg* or *Aplnr*.[38] These results may suggest that animal models of PVOD, based on the deletion of *Erg* or *Aplnr*, may induce pulmonary venous lesions independently of the *EIF2AK4* pathway, the main predisposing gene factor for heritable PVOD.[4] Relations between exposure to the alkylating agent *EIF2AK4* and the ERG-APLN axis should better characterize the pathophysiology of PVOD. Interestingly, *Erg-Aplnr*–related and MMC-induced PVOD models may allow us to address distinct aspects of PVOD. The first model is a model of pulmonary venular sprouting, whereas the second is an Eif2ak4-related model that reproduces the whole spectrum of PVOD lesions.

In conclusion, 7 cases of MMC-induced PVOD were identified in the French PH Network in a 3-year period. Physicians should be aware of this rare complication of MMC therapy. Unexplained dyspnea after MMC therapy should raise the possibility of underlying pulmonary vascular toxicity and PVOD should be screened for through a noninvasive workup (diffusing capacity of the lung for carbon monoxide, blood gases, Doppler echocardiography, and a high-resolution CT of the chest). Possible cases of PVOD at screening should undergo right heart catheterization to confirm and evaluate PH severity. Our preclinical data confirm the links between MMC exposure and pulmonary venous lesions, and open up a new area of research. MMC-induced PVOD in rats is a novel animal model for human PVOD, which allows us to test innovative strategies to prevent and treat this devastating disease. Amifostine prevents MMC-induced PVOD in rats and should be tested as a preventive therapy of MMC-induced PVOD in humans.

Acknowledgments

We acknowledge the French pulmonary hypertension pharmacovigilance network, VIGIAPATH, supported by the Agence Nationale de Sécurité du Médicament et des Produits de Santé (ANSM). The authors thank Newmed Publishing for editing the article. The authors thank Pr Florent Soubrier and Dr Mélanie Eyries for genetic screening of *BMPR2* and *EIF2AK4* mutations.

Sources of Funding

Dr Perros receives funding from National Funding Agency for Research (ANR; grant ANR-13-JSV1-001). Dr Ranchoux is supported by the LabEx LERMIT. Dr Hautefort is supported by a PhD grant from Région Ile de France (CORDDIM). Dr Antigny is supported by a postdoctoral grant from Aviesan (ITMO IHP). Dr Godinas is supported from the European Respiratory Society (grant LTRF-2013-1592).

Disclosures

Drs Günther, Savale, Jaïs, Sitbon, Cottin, Simonneau, Humbert, and Montani have relationships with drug companies including Actelion, Bayer, GSK, Novartis, and Pfizer. In addition to being investigators in trials involving these companies, other relationships include consultancy services and memberships of scientific advisory boards. The other authors report no conflicts.

References

1. Montani D, Price LC, Dorfmuller P, Achouh L, Jaïs X, Yaïci A, Sitbon O, Musset D, Simonneau G, Humbert M. Pulmonary veno-occlusive disease. *Eur Respir J*. 2009;33:189–200. doi: 10.1183/09031936.00090608.
2. Mandel J, Mark EJ, Hales CA. Pulmonary veno-occlusive disease. *Am J Respir Crit Care Med*. 2000;162:1964–1973. doi: 10.1164/ajrccm.162.5.9912045.
3. Wagenvoort CA, Wagenvoort N. Primary pulmonary hypertension: a pathologic study of the lung vessels in 156 clinically diagnosed cases. *Circulation*. 1970;42:1163–1184.
4. Eyries M, Montani D, Girerd B, Perret C, Leroy A, Lonjou C, Chelghoum N, Coulet F, Bonnet D, Dorfmüller P, Fadel E, Sitbon O, Simonneau G, Tregouët DA, Humbert M, Soubrier F. EIF2AK4 mutations cause pulmonary veno-occlusive disease, a recessive form of pulmonary hypertension. *Nat Genet*. 2014;46:65–69. doi: 10.1038/ng.2844.
5. Joselson R, Warnock M. Pulmonary veno-occlusive disease after chemotherapy. *Hum Pathol*. 1983;14:88–91.
6. Ranchoux B, Günther S, Quarck R, Chaumais M-C, Dorfmüller P, Antigny F, Dumas SJ, Raymond N, Lau E, Savale L, Jais X, Simonneau G, Stenmark K, Cohen-Kaminsky S, Humbert M, Montani D, Perros F. Chemotherapy-induced pulmonary hypertension: role of alkylating agents. *Am J Pathol*. 2015;185:356–71.
7. Humbert M, Sitbon O, Chaouat A, Bertocchi M, Habib G, Gressin V, Yaïci A, Weitzenblum E, Cordier JF, Chabot F, Dromer C, Pison C, Reynaud-Gaubert M, Haloun A, Laurent M, Hachulla E, Cottin V, Degano B, Jaïs X, Montani D, Souza R, Simonneau G. Survival in patients with idiopathic, familial, and anorexigen-associated pulmonary arterial hypertension in the modern management era. *Circulation*. 2010;122:156–163. doi: 10.1161/CIRCULATIONAHA.109.911818.
8. Humbert M, Sitbon O, Yaïci A, Montani D, O'Callaghan DS, Jaïs X, Parent F, Savale L, Natali D, Günther S, Chaouat A, Chabot F, Cordier JF, Habib G, Gressin V, Jing ZC, Souza R, Simonneau G; French Pulmonary Arterial Hypertension Network. Survival in incident and prevalent cohorts of patients with pulmonary arterial hypertension. *Eur Respir J*. 2010;36:549–555. doi: 10.1183/09031936.00057010.
9. Humbert M, Sitbon O, Chaouat A, Bertocchi M, Habib G, Gressin V, Yaici A, Weitzenblum E, Cordier JF, Chabot F, Dromer C, Pison C, Reynaud-Gaubert M, Haloun A, Laurent M, Hachulla E, Simonneau G. Pulmonary arterial hypertension in France: results from a national registry. *Am J Respir Crit Care Med*. 2006;173:1023–1030. doi: 10.1164/rccm.200510-1668OC.
10. Sitbon O, Humbert M, Jaïs X, Ioos V, Hamid AM, Provencher S, Garcia G, Parent F, Hervé P, Simonneau G. Long-term response to calcium channel blockers in idiopathic pulmonary arterial hypertension. *Circulation*. 2005;111:3105–3111. doi: 10.1161/CIRCULATIONAHA.104.488486.
11. Urboniene D, Haber I, Fang YH, Thenappan T, Archer SL. Validation of high-resolution echocardiography and magnetic resonance imaging vs. high-fidelity catheterization in experimental pulmonary hypertension. *Am J Physiol Lung Cell Mol Physiol*. 2010;299:L401–L412. doi: 10.1152/ajplung.00114.2010.
12. Rudski LG, Lai WW, Afilalo J, Hua L, Handschumacher MD, Chandrasekaran K, Solomon SD, Louie EK, Schiller NB. Guidelines for the echocardiographic assessment of the right heart in adults: a report from the American Society of Echocardiography endorsed by the European Association of Echocardiography, a registered branch of the European Society of Cardiology, and the Canadian Society of Echocardiography. *J Am Soc Echocardiogr*. 2010;23:685–713; quiz 786. doi: 10.1016/j.echo.2010.05.010.
13. Perros F, Dorfmüller P, Souza R, Durand-Gasselin I, Mussot S, Mazmanian M, Hervé P, Emilie D, Simonneau G, Humbert M. Dendritic cell recruitment in lesions of human and experimental pulmonary hypertension. *Eur Respir J*. 2007;29:462–468. doi: 10.1183/09031936.00094706.
14. Chesné J, Danger R, Botturi K, Reynaud-Gaubert M, Mussot S, Stern M, Danner-Boucher I, Mornex JF, Pison C, Dromer C, Kessler R, Dahan M, Brugière O, Le Pavec J, Perros F, Humbert M, Gomez C, Brouard S, Magnan A; COLT Consortium. Systematic analysis of blood cell transcriptome in end-stage chronic respiratory diseases. *PLoS One*. 2014;9:e109291. doi: 10.1371/journal.pone.0109291.
15. Abramowitz L, Rémy V, Vainchtock A. Economic burden of anal cancer management in France. *Rev Epidemiol Sante Publique*. 2010;58:331–338. doi: 10.1016/j.respe.2010.06.165.
16. Sztrymf B, Coulet F, Girerd B, Yaici A, Jais X, Sitbon O, Montani D, Souza R, Simonneau G, Soubrier F, Humbert M. Clinical outcomes of pulmonary arterial hypertension in carriers of BMPR2 mutation. *Am J Respir Crit Care Med*. 2008;177:1377–1383. doi: 10.1164/rccm.200712-1807OC.
17. Knight BK, Rose AG. Pulmonary veno-occlusive disease after chemotherapy. *Thorax*. 1985;40:874–875.
18. Gagnadoux F, Capron F, Lebeau B. Pulmonary veno-occlusive disease after neoadjuvant mitomycin chemotherapy and surgery for lung carcinoma. *Lung Cancer*. 2002;36:213–215.
19. Swift GL, Gibbs A, Campbell IA, Wagenvoort CA, Tuthill D. Pulmonary veno-occlusive disease and Hodgkin's lymphoma. *Eur Respir J*. 1993;6:596–598.
20. Waldhorn RE, Tsou E, Smith FP, Kerwin DM. Pulmonary veno-occlusive disease associated with microangiopathic hemolytic anemia and chemotherapy of gastric adenocarcinoma. *Med Pediatr Oncol*. 1984;12:394–396.
21. Okuno SH, Frytak S. Mitomycin lung toxicity. Acute and chronic phases. *Am J Clin Oncol*. 1997;20:282–284.
22. Curado MP, International Agency for Research on Cancer, International Association of Cancer Registries. *Cancer incidence in five continents*, Volume IX. Lyon; Geneva: International Agency for Research on Cancer ; Distributed by WHO Press, World Health Organization; 2008.
23. Savale L, Chaumais MC, Cottin V, Bergot E, Frachon I, Prevot G, Pison C, Dromer C, Poubeau P, Lamblin N, Habib G, Reynaud-Gaubert M, Bourdin A, Sanchez O, Tubert-Bitter P, Jaïs X, Montani D, Sitbon O, Simonneau G, Humbert M. Pulmonary hypertension associated with benfluorex exposure. *Eur Respir J*. 2012;40:1164–1172. doi: 10.1183/09031936.00188611.
24. Montani D, Bergot E, Günther S, Savale L, Bergeron A, Bourdin A, Bouvaist H, Canuet M, Pison C, Macro M, Poubeau P, Girerd B, Natali D, Guignabert C, Perros F, O'Callaghan DS, Jaïs X, Tubert-Bitter P, Zalcman G, Sitbon O, Simonneau G, Humbert M. Pulmonary arterial hypertension in patients treated by dasatinib. *Circulation*. 2012;125:2128–2137. doi: 10.1161/CIRCULATIONAHA.111.079921.
25. Montani D, Achouh L, Dorfmüller P, Le Pavec J, Sztrymf B, Tchérakian C, Rabiller A, Haque R, Sitbon O, Jaïs X, Dartevelle P, Maître S, Capron F, Musset D, Simonneau G, Humbert M. Pulmonary veno-occlusive disease: clinical, functional, radiologic, and hemodynamic characteristics and outcome of 24 cases confirmed by histology. *Medicine (Baltimore)*. 2008;87:220–233. doi: 10.1097/MD.0b013e31818193bb.
26. Humbert M, Maître S, Capron F, Rain B, Musset D, Simonneau G. Pulmonary edema complicating continuous intravenous prostacyclin in pulmonary capillary hemangiomatosis. *Am J Respir Crit Care Med*. 1998;157(5 pt 1):1681–1685. doi: 10.1164/ajrccm.157.5.9708065.
27. Task Force for Diagnosis and Treatment of Pulmonary Hypertension of European Society of Cardiology (ESC), European Respiratory Society (ERS), International Society of Heart and Lung Transplantation (ISHLT), Galiè N, Hoeper MM, Humbert M, Torbicki A, Vachiery J-L, Barbera JA, Beghetti M, Corris P, Gaine S, Gibbs JS, Gomez-Sanchez MA, Jondeau G, Klepetko W, Opitz C, Peacock A, Rubin L, Zellweger M, Simonneau

G. Guidelines for the diagnosis and treatment of pulmonary hypertension. *Eur Respir J*. 2009;34:1219–1263.
28. Bradner WT. Mitomycin C: a clinical update. *Cancer Treat Rev*. 2001;27:35–50. doi: 10.1053/ctrv.2000.0202.
29. Hoorn CM, Wagner JG, Petry TW, Roth RA. Toxicity of mitomycin C toward cultured pulmonary artery endothelium. *Toxicol Appl Pharmacol*. 1995;130:87–94. doi: 10.1006/taap.1995.1012.
30. Verweij J, van Zanten T, Souren T, Golding R, Pinedo HM. Prospective study on the dose relationship of mitomycin C-induced interstitial pneumonitis. *Cancer*. 1987;60:756–761.
31. Siegel D, Franklin WA, Ross D. Immunohistochemical detection of NAD(P)H:quinone oxidoreductase in human lung and lung tumors. *Clin Cancer Res*. 1998;4:2065–2070.
32. Gatzemeier U, Fasske E, Nowak U. Experimental and clinical data of the pulmonary toxicity of mitomycin C [in German]. *Pneumologie*. 1990;44(suppl 1):201–203.
33. Schraufnagel DE, Sekosan M, McGee T, Thakkar MB. Human alveolar capillaries undergo angiogenesis in pulmonary veno-occlusive disease. *Eur Respir J*. 1996;9:346–350.
34. Ruiter G, de Man FS, Schalij I, Sairras S, Grünberg K, Westerhof N, van der Laarse WJ, Vonk-Noordegraaf A. Reversibility of the monocrotaline pulmonary hypertension rat model. *Eur Respir J*. 2013;42:553–556. doi: 10.1183/09031936.00012313.
35. Duperray A, Tranqui L, Alix JL, Cordonnier D. Effect of mitomycin C on prostacyclin synthesis by human endothelial cells. *Biochem Pharmacol*. 1988;37:4753–4757.
36. Rockwell S. Cytotoxicities of mitomycin C and x rays to aerobic and hypoxic cells *in vitro*. *Int J Radiat Oncol Biol Phys*. 1982;8:1035–1039.
37. Wilson GJ, Bunpo P, Cundiff JK, Wek RC, Anthony TG. The eukaryotic initiation factor 2 kinase GCN2 protects against hepatotoxicity during asparaginase treatment. *Am J Physiol Endocrinol Metab*. 2013;305:E1124–E1133. doi: 10.1152/ajpendo.00080.2013.
38. Lathen C, Zhang Y, Chow J, Singh M, Lin G, Nigam V, Ashraf YA, Yuan JX, Robbins IM, Thistlethwaite PA. ERG-APLNR axis controls pulmonary venule endothelial proliferation in pulmonary veno-occlusive disease. *Circulation*. 2014;130:1179–1191. doi: 10.1161/CIRCULATIONAHA.113.007822.

CLINICAL PERSPECTIVE

Pulmonary veno-occlusive disease (PVOD) is a rare form of pulmonary hypertension characterized by a progressive occlusion of the small pulmonary veins by fibrous tissue and intimal thickening. Recently, biallelic mutations in the eukaryotic translation initiation factor 2-αkinase 4 (*EIF2AK4)* gene have been demonstrated as the major genetic cause of heritable PVOD. Apart from genetic predisposition, other risk factors have also been identified including cases induced by chemotherapeutic agents. In the present study, we report 7 new cases of mitomycin-C–induced PVOD identified in the French Pulmonary Hypertension Registry and reported to the French pharmacovigilance agency. All patients had a history of squamous anal cancer and were treated with mitomycin-C alone or in association with 5-fluorouracil. The estimated annual incidence of PVOD in the French population with anal cancer was 3.9 of 1000 patients, which is much higher than the incidence of PVOD in the general population (0.5/million per year). Physicians should thus be aware of this rare complication of mitomycin-C therapy, and unexplained dyspnea in this condition should raise the possibility of underlying pulmonary vascular toxicity. In addition, intraperitoneal administration of mitomycin-C induced PVOD in rats, as demonstrated by pulmonary hypertension at right heart catheterization with major remodeling of small pulmonary veins and foci of intense microvascular endothelial-cell proliferation of the capillary bed. This was associated with a reduced pulmonary expression of GCN2, the protein coded by *EIF2AK4* gene. This animal model mimicking human PVOD opens up a new area of research and represents a unique opportunity to test innovative strategies in this devastating disease.

Mitomycin-Induced Pulmonary Veno-Occlusive Disease: Evidence From Human Disease and Animal Models

Frédéric Perros, Sven Günther, Benoit Ranchoux, Laurent Godinas, Fabrice Antigny, Marie-Camille Chaumais, Peter Dorfmüller, Aurélie Hautefort, Nicolas Raymond, Laurent Savale, Xavier Jaïs, Barbara Girerd, Vincent Cottin, Olivier Sitbon, Gerald Simonneau, Marc Humbert and David Montani

Circulation. 2015;132:834-847; originally published online June 30, 2015;
doi: 10.1161/CIRCULATIONAHA.115.014207
Circulation is published by the American Heart Association, 7272 Greenville Avenue, Dallas, TX 75231

Print ISSN: 0009-7322. Online ISSN: 1524-4539

SUPPLEMENTAL MATERIAL

Expanded Methods

In vivo study design

Rats were housed at the Faculty of Pharmacy of Châtenay-Malabry (ANIMEX platform, Châtenay Malabry, France). Experiments were conducted according to the European Union regulations (Directive 86/609 EEC) for animal experiments and complied with our institution's guidelines for animal care and handling. The animal facility is licensed by the French Ministry of Agriculture (agreement N° B92-019-01). This study was approved by the Committee on the Ethics of Animal Experiments CEEA26 CAP Sud. Animal experiments were supervised by Dr. Frederic Perros (agreement delivered by the French Ministry of Agriculture for animal experiment N° A92–392). All efforts were made to minimize animal suffering.

Male and female Wistar rats (Janvier, eight weeks old) were subjected to different protocols to evaluate sex differences, dose–response relationships and the kinetics of PH development after MMC exposure.

Protocol 1: Gender-specific susceptibility. Male and female rats were randomly divided into saline (control, *n*=5) or MMC-exposed groups (Ametycin, Sanofi, 4 mg/kg, i.p., *n*=10). We performed haemodynamic measurements, assessed right-ventricle hypertrophy and tissues were collected at 24 days after the injection.

Protocol 2: Dose–response relationships. Females, which harboured a more severe response to MMC (than males), were used to study MMC-induced severe pulmonary vasculopathy induced by fractioned lower doses. Rats were randomly divided into saline (control, *n*=5) or MMC-exposed groups: i.e., 2 and 3 mg/kg/week/2 weeks (i.p. *n*=10 for each dose). Rats were sacrificed at 30 days after the first injection. Haemodynamic measurements were made, right-ventricle hypertrophy was assessed and tissue samples were collected.

Protocol 3: Kinetics of PH development. Female rats were randomly divided into saline (control, *n*=5) or MMC-exposed groups (3 mg/kg/week/2 weeks, i.p., *n*=10). We evaluated the haemodynamics using echocardiography at baseline, and at 1, 2, 3, 4 and 5 weeks after the first MMC injection (*n*=5–10 rats for each time point).

Protocol 4: Prevention study. Amifostine was given i.p. at 200mg/kg 30 minutes prior to 3 mg/kg/week/2 weeks of MMC (n=15). This group was compared to MMC only-exposed group (MMC, 3 mg/kg/week/2 weeks,

n=25). Survival was evaluated over five weeks. Survivors were sacrificed five weeks after the second CP injection for hemodynamic, RVH measurements, and tissue collection.

Regarding the doses used in this study, Warren et al[1] used MMC-DNA adducts as an indicator for the host's exposure and capacity for metabolic activation, detoxification, and DNA repair. In mice, they found that MMC (4 mg/kg) was roughly equivalent to a conventional human chemotherapy dose. In rats, Mizushima et al[2] found that 2, 3, and 4 mg/kg MMC induced 0, 33 and 30% mortality, respectively at 28 days. Those doses corresponded in this species, to high-dose chemotherapy. We decided to use 4 mg/kg and lower (3 and 2 mg/kg) in rats as they seemed to be in the equivalent range of human chemotherapy.

As addressed by Andreollo et al[3], the differences in anatomy, physiology, development and biological phenomena must be taken into consideration when comparing time-lapse between rat and human. Rats rapidly develop during childhood and become sexually mature at about six weeks old, but reach social maturity five to six months later. In adulthood, every month of the animal is approximately equivalent to 2.5 human years. Several authors performed experimental studies in rats and estimated 30 days of human life for everyday life of the animal[3]. Regarding our observations in humans, the delay between initiation of MMC therapy and final diagnosis of PVOD was 5.3 months (range: 2–12 months). It is difficult to compare the development of pulmonary vascular damage in animals and in humans, but in each case the development of PVOD after exposure to chemotherapeutical drugs is rapid.

Quantification of pulmonary microvessels neomuscularization

OCT-embedded frozen lungs were sectioned at 6 µm thickness and stained in double immunofluorescence, for von Willebrand factor (vWF, Dako) and α-smooth muscle actin (α-SMA, clone 1A4, Sigma). 40 to 60 pulmonary microvessels (<50µm) were analyzed and categorized as muscularized when vWF+ endothelial cells in microvessels were coated with α-SMA+ smooth muscle cells (fully [FM] or partially [PM] when vessels contained at least one cell that was positive for α-SMA but lacked a continuous layer) or non-muscularized (NM) in the absence of this coating, to assess the degree of muscularization of these normally non-muscularized pre- and post-capillary vessels.

Supplementary legends and figures

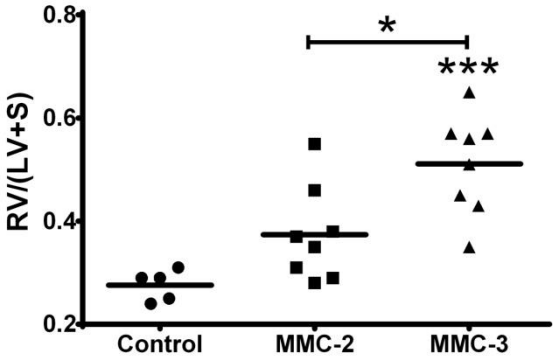

Supplementary figure 1: MMC induces PH in a dose-dependent manner. Female rats harboured a more severe response to MMC than males: thus, they were chosen to study MMC-induced severe pulmonary vasculopathy after fractioned lower doses of MMC (2 and 3 mg/kg at one week apart). Rats exposed twice to MMC were too fragile to undergo invasive haemodynamic measurements, so we quantified PH though the Fulton Index =RV/(LV+S) at 30 days after the first injection. Rats exposed to the higher dose of MMC had more severe right-ventricular hypertrophy than those exposed to the lower dose.

Dot plots with means; *: *P*<0.05, ***: *P*<0.001

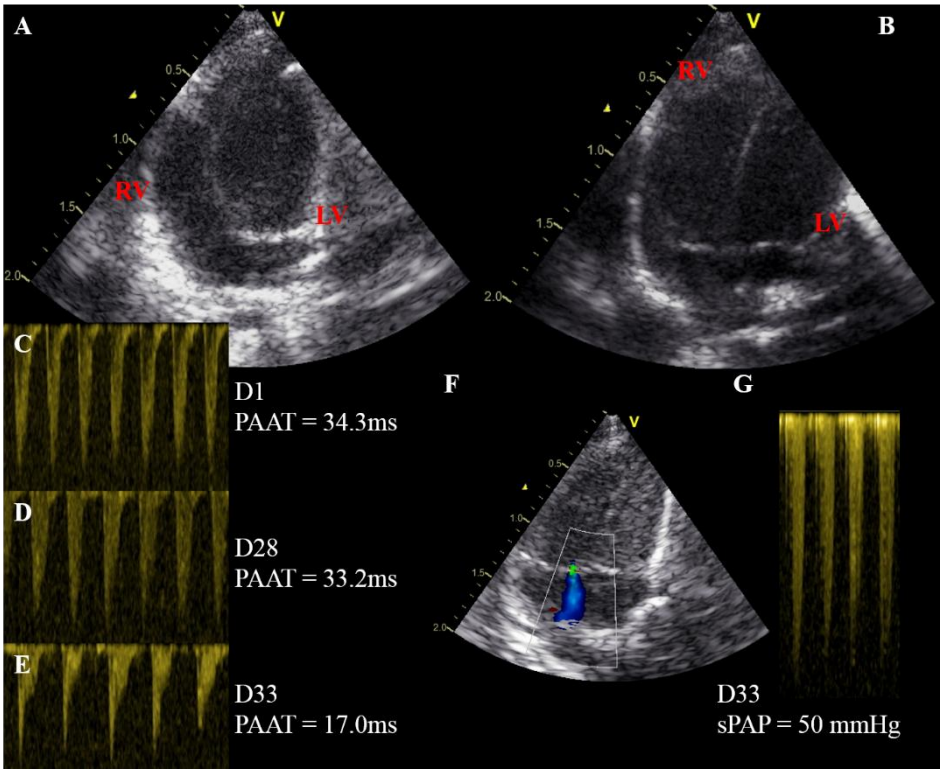

Supplementary figure 2: MMC exposed rat displaying features of PH. A. Four chambers view at day 28 with ratio RV/LV < 1. B. Four chambers view of the same rat at day 33 with a RV/LV ratio > 1. C. Pulmonary artery

acceleration time at day 1 (34.3 ms). D. Pulmonary artery acceleration time at day 28 (33.2 ms). E. Pulmonary artery acceleration time at day 33 (17.0) with mid-systolic notch. Velocity-time integral allowed an estimation of cardiac output of 45.1ml/min. F. At day 33, a tricuspid regurgitation jet appeared. G. The sPAP estimated with tricuspid regurgitation jet was 50 mm Hg. Right heart catheterization in the same rat has given: sPAP/dPAP/mPAP as follow 49/13/31 mm Hg and CO of 45.6 ml/min.

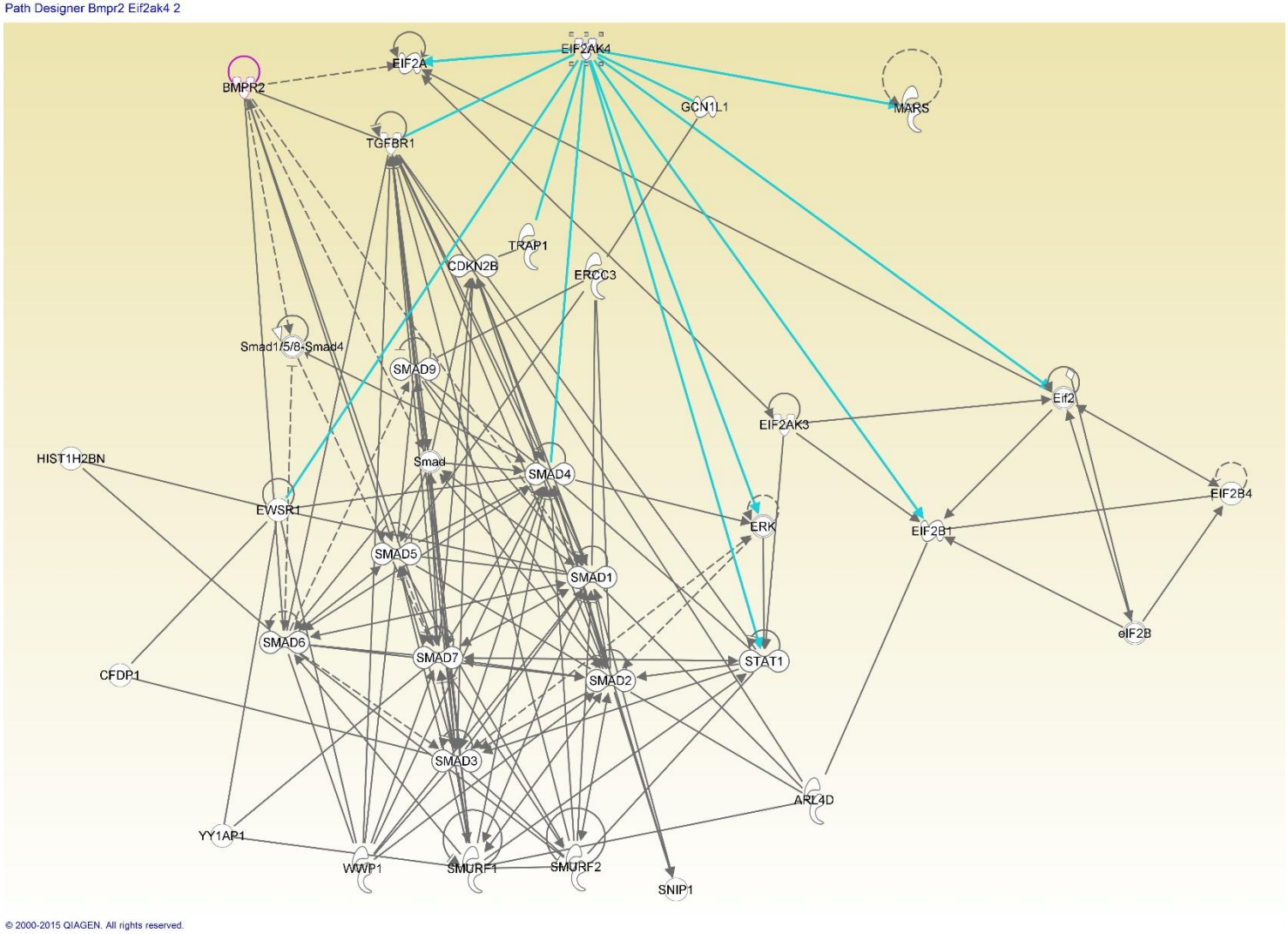

Supplementary figure 3: Network analysis using Ingenuity pathway analysis (IPA) software. This figure depicts the merged networks of proteins/molecules belonging to the BMPRII (*BMPR2* gene), and GCN2 (*EIF2AK4* gene) signaling. IPA analysis highlights complex and unrevealed interplay between both signaling. Genes/proteins implicated in this network:

ARL4D:	ADP-ribosylation factor-like 4D
BMPR2:	bone morphogenetic protein receptor, type II (serine/threonine kinase)
CDKN2B:	cyclin-dependent kinase inhibitor 2B (p15, inhibits CDK4)
CFDP1:	craniofacial development protein 1
Eif2:	eIF2, Initiation Factor M1

EIF2A:	eukaryotic translation initiation factor 2A, 65kDa
EIF2AK3:	eukaryotic translation initiation factor 2-alpha kinase 3
EIF2AK4:	eukaryotic translation initiation factor 2 alpha kinase 4
EIF2B1:	eukaryotic translation initiation factor 2B, subunit 1 alpha, 26kDa
EIF2B4:	eukaryotic translation initiation factor 2B, subunit 4 delta, 67kDa
ERCC3:	excision repair cross-complementation group 3
ERK:	p42/44 mapk
EWSR1:	EWS RNA-binding protein 1
GCN1L1:	GCN1 general control of amino-acid synthesis 1-like 1 (yeast)
HIST1H2BN:	histone cluster 1, H2bn
MARS:	methionyl-tRNA synthetase
SMAD1:	SMAD family member 1
SMAD2:	SMAD family member 2
SMAD3:	SMAD family member 3
SMAD4:	SMAD family member 4
SMAD5:	SMAD family member 5
SMAD6:	SMAD family member 6
SMAD7:	SMAD family member 7
SMAD9:	SMAD family member 9
SMURF1:	SMAD specific E3 ubiquitin protein ligase 1
SMURF2:	SMAD specific E3 ubiquitin protein ligase 2
SNIP1:	Smad nuclear interacting protein 1
STAT1:	signal transducer and activator of transcription 1, 91kDa
TGFBR1:	transforming growth factor, beta receptor 1
TRAP1:	TNF receptor-associated protein 1
WWP1:	WW domain containing E3 ubiquitin protein ligase 1
YY1AP1:	YY1 associated protein 1

1. Warren AJ, Mustra DJ, Hamilton JW. Detection of mitomycin C-DNA adducts in human breast cancer cells grown in culture, as xenografted tumors in nude mice, and in biopsies of human breast cancer patient tumors as determined by (32)P-postlabeling. *Clin Cancer Res Off J Am Assoc Cancer Res*. 2001;7:1033–1042.

2. Mizushima Y, Morikage T, Sasaki K, Yano S. Most effective route of administration and utilization of high-dose chemotherapy with bone marrow transplantation in rats. *Cancer Res*. 1989;49:2561–2566.

3. Andreollo NA, Santos EF dos, Araújo MR, Lopes LR. Rat's age versus human's age: what is the relationship? *Arq Bras Cir Dig ABCD Braz Arch Dig Surg*. 2012;25:49–51.